UNIVERSIDADE FEDERAL DO CEARÁ
CENTRO DE TECNOLOGIA
CURSO DE ENGENHARIA DE PETRÓLEO

LIGIA TORNISIELLO

A MODEL FOR PRELIMINARY DESIGN OF STEEL CATENARY RISERS USING BIO-INSPIRED ALGORITHMS

FORTALEZA

2017

LIGIA TORNISIELLO

A MODEL FOR PRELIMINARY DESIGN OF STEEL CATENARY RISERS USING BIO-INSPIRED ALGORITHMS

Monography presented in the undergraduate course of Petroleum Engineering of the Centro de Tecnologia of Universidade Federal do Ceará, as a partial requirement for obtaining the title of Bachelor of Petroleum Engineering.

Supervisor: Evandro Parente Junior

FORTALEZA

2017

Dados Internacionais de Catalogação na Publicação
Universidade Federal do Ceará
Biblioteca Universitária
Gerada automaticamente pelo módulo Catalog, mediante os dados fornecidos pelo(a) autor(a)

T638m Tornisiello, Ligia.
A model for preliminary design of steel catenary risers using bio-inspired algorithms / Ligia Tornisiello. – 2017.
79 f. : il. color.

Trabalho de Conclusão de Curso (graduação) – Universidade Federal do Ceará, Centro de Tecnologia, Curso de Engenharia de Petróleo, Fortaleza, 2017.
Orientação: Prof. Dr. Evandro Parente Junior.

1. Risers. 2. Otimização. 3. Algoritmos bio-inspirados. I. Título.

CDD 665.5092

LIGIA TORNISIELLO

A MODEL FOR PRELIMINARY DESIGN OF STEEL CATENARY RISERS USING BIO-INPIRED ALGORITHMS

Monography presented in the undergraduate course of Petroleum Engineering of the Centro de Tecnologia of Universidade Federal do Ceará, as a partial requirement for obtaining the title of Bachelor of Petroleum Engineering.

Approved on: ___/___/_____.

EXAMINING BOARD

Prof. Evandro Parente Junior, Dr. (Supervisor)
Universidade Federal do Ceará (UFC)

Prof. Antônio Macário Cartaxo de Melo, Dr.
Universidade Federal do Ceará (UFC)

Prof. Pedro Felipe Gadelha Silvino, MSc.
Universidade Federal do Ceará (UFC)

To God.

To my parents, Nivaldo and Leni, for their endless love.

ACKNOWLEDGEMENTS

To my parents, José Nivaldo Tornisiello and Leni Aparecida Sbravatti, who have always believed in my potential and supported me in all decisions during my academic life. I salute you for the confidence, encouragement, for providing me good education and teaching me the value of hardwork. To my brother, Rodrigo, for the friendship.

To my boyfriend, Bruno, for the companionship and motivation throughout these years and for the opportunity of sharing great experiences, from the exchange studies to the leadership of the board of directors of the Society of Petroleum Engineers student chapter at UFC.

To my supervisor, Evandro Parente Junior, for all the knowledge transmitted along the eighteen months of development of the research and for the excellent orientation.

To the professors of the examining board, Antônio Macário Cartaxo de Melo and Pedro Felipe Gadelha Silvino.

To the colleagues of Laboratório de Mecânica Computacional e Visualização (LMCV), in special, Juliana, Elias, Guilherme, Luana and Marina who directly helped me in some stage of the development of this research.

To CNPq and ANP/UFC PRH-31 for the financial support.

To CAPES and the Ministry of Education of Brazil, for the scholarship that I was granted. The experiences lived at Missouri University of Science and Technology and at the University of Texas at Austin were fundamental to improvement in technical knowledge and likewise important to my personal growth and maturity.

To my classmates, Lara, Milena, Bruna, Matheus and Renan, for the moments shared during the disciplines and entertainment outside of the class.

"If four things are followed – having a great aim, acquiring knowledge, hard work, and perseverance – then anything can be achieved."

A. P. J. Abdul Kalam

ABSTRACT

Risers are tubular structures used in offshore production systems to convey the fluids from the wellhead at the seabed to a floating platform on the sea surface. They can be fabricated with distinct materials, from various grades of steel to titanium and composite materials. Furthermore, these structures can be installed in different configurations, from free-hanging catenary to configurations that include floating elements. Independent of the material and configuration, all risers are subjected to diverse types of loadings, including hydrostatic internal and external pressures, weight and buoyancy, weight of internal fluid, waves, currents, and vessel motion. The design of a riser is very time consuming, since a large number of parameters (e.g. thickness, top angle, and material properties) are involved and tight safety requirements must be met. This leads to the study of tools, such as optimization algorithms, that can speed up the process of elaborating a feasible riser design for certain conditions. Considering that some of the parameters in the design of a riser can assume a discrete set of values, the utilization of mathematical programming algorithms becomes unfeasible. It is then necessary to use metaheuristic algorithms, such as Genetic Algorithm (GA) and Particle Swarm Optimization (PSO). In this context, this work presents a study on the application of bio-inspired algorithms, including GA and PSO, to the design optimization of steel catenary risers. The problem consists of finding the riser material and wall thickness that minimize the riser cost, in conformance with the requirements of technical standards. An inextensible cable model is utilized for riser analysis in the static and quasi-static loading cases. Based on the potential of the association of surrogate models with optimization algorithms, a surrogate model for the prediction of the dynamic amplification factor was developed in this work to be utilized in lieu of dynamic analysis. The main hypotheses that were adopted are presented, along with the description of the methodology employed for the construction of the surrogate model, including the selection of the variables, the design of the experiments, model training and validation. The efficiency of the utilized algorithms in finding an optimum riser design for the specified conditions is confirmed by the obtained numerical results. Assuredly, the main contribution of this work is the development of a model for preliminary design of steel catenary risers that reduces the dependence on the designer's experience and allows this activity to be conducted within an acceptable execution time.

Keywords: Risers. Optimization. Bio-inspired algorithms.

RESUMO

Risers são estruturas tubulares utilizadas em sistemas de produção de petróleo offshore para transportar os fluidos produzidos da cabeça do poço no solo marinho a uma unidade flutuante no nível do mar. Essas estruturas podem ser fabricadas com diferente materiais, incluindo diversos tipos de aço, titânio e materiais compósitos, e instalados em diversas configurações, desde catenária livre a configurações que incluem elementos flutuantes. Independente do material e configuração, todos os risers estão sujeitos a diversos carregamentos, incluindo pressão hidrostática interna e externa, peso próprio e empuxo, ondas, correntes e movimento da plataforma (offset). O projeto de um riser envolve muitos parâmetros, considerando também aspectos relacionados a segurança. Então, a seleção de um riser com desempenho estrutural aceitável para determinado cenário pode se tornar um processo exaustivo, e, portanto, deve ser tratado como um problema de otimização. A utilização de algoritmos de programação matemática não é viável nesse caso, pois alguns dos parâmetros do design de um riser podem assumir valores discretos. É necessário então utilizar algoritmos metaheuristicos, como Algoritmos Genéticos (AG) e Otimização por Enxame de Partículas (PSO). Nesse contexto, esse trabalho apresenta um estudo da aplicação de algoritmos bio-inspirados, incluindo AG e PSO, para otimização de risers de aço em catenária. O problema consiste em encontrar o material e espessura de parede que minimizam o custo do riser, em conformidade com os requerimentos de normas técnicas. A análise do riser nos casos de carga estáticos e quase-estáticos é feita utilizando um modelo de cabo inextensível. Baseado no potencial de associação de metamodelos e algoritmos de otimização, um metamodelo para previsão do fator de amplificação dinâmica foi elaborado nesse trabalho para substituir as análises dinâmicas. As hipóteses adotadas serão apresentadas, juntamente com a descrição da metodologia para elaboração do metamodelo, incluindo a seleção das variáveis, o projeto de experimentos, treinamento e validação do modelo. A eficiência dos algoritmos em encontrar um projeto ótimo de riser para as condições especificadas é confirmada com os resultados dos exemplos numéricos. Certamente, a maior contribuição desse trabalho foi a elaboração de um modelo para projeto preliminar de riser de aço em catenária que reduz a dependência da experiência do projetista nessa atividade e permite que o pré-dimensionamento seja realizado em um tempo de execução aceitável.

Palavras-chave: Risers. Otimização. Algoritmos bio-inspirados.

LIST OF FIGURES

LIST OF TABLES

LIST OF ABBREVIATIONS AND ACRONYMS

ABS	American Bureau of Shipping
AFFG	Adaptive Fuzzy Fitness Granulation
AIS	Artificial Immune System
ALS	Accidental Limit State
ANN	Artificial Neural Networks
API	American Petroleum Institute
ASME	American Society of Mechanical Engineers
CAPEX	Capital Expenditures
DNV	Det Noske Veritas
FEED	Front-end Engineering Design
FEM	Finite Element Model
FLS	Fatigue Limit State
FPSO	Floating Production Storage and Offloading
FSHR	Free Standing Hybrid Riser
GA	Genetic Algorithm
HPHT	High Pressure High Temperature
IGA	Island-based Genetic Algorithm
ISO	International Standardization Organisation
LFRD	Load and Resistance Factor Design
LHS	Latin Hypercube Sampling
MAE	Maximum Absolute Error
MARS	Multivariate Adaptive Regression Splines
MIGA	Multi-island Genetic Algorithm
NLPQL	Non-linear Programming by Quadratic Lagrangian
NSGA-II	Non-dominated Sorting Genetic Algorithm II
OOP	Object-Oriented Programming
PF	Penalty Function
PSO	Particle Swarm Optimization
RAO	Response Amplitude Operator
RBDO	Reliability-based Design Optimization
RBF	Radial Basis Functions

RMSE	Root Mean Squared Error
SCR	Steel Catenary Riser
SLS	Serviceability Limit State
SQP	Sequential Quadratic Programming
SVM	Support Vector Machine
TDP	Touchdown Point
TDZ	Touchdown Zone
ULS	Ultimate Limit State
VIV	Vortex Induced Vibration
WSD	Working Stress Design

LIST OF SYMBOLS

D	riser out diameter
C_i	relative cost of the material
E	Young's modulus
f_o	ovality
f_u	tensile strength
$f_{u,temp}$	temperature derating factor for the tensile strength
f_y	yield strength
$f_{y,temp}$	temperature derating factor for the yield stress
g	gravity acceleration
h	hydrostatic column at the specified riser cross section
L_i	length or the riser segment
M_A	bending moment from accidental loads
M_d	design bending moment
M_E	bending moment from environmental loads
M_F	bending moment from functional loads
M_k	plastic bending moment resistance
n	number of riser segments
P_b	burst resistance
P_c	hoop buckling resistance
P_d	design pressure
P_e	external pressure
P_{el}	elastic collapse pressure
P_{ld}	local internal design pressure
P_{li}	local incidental pressure
P_{min}	minimum internal pressure
P_p	plastic collapse pressure
P_{Pr}	resistance against buckling propagation
R_e	external radius of the riser segment
R_i	internal radius of the riser segment
SMTS	specified minimum tensile strength at room temperature
SMYS	specified minimum yield stress at room temperature

SWL	still water level
t	riser wall thickness
T_{eA}	effective tension from accidental loads
T_{ed}	design effective tension
T_{eE}	effective tension from environmental loads
T_{eF}	effective tension from functional loads
T_k	plastic axial force resistance
α_c	parameter accounting for strain hardening and wall thinning
α_{fab}	fabrication factor
α_U	material strength factor
γ_A	load effect factor for accidental loads
γ_c	buckle propagation factor
γ_E	load effect factor for environmental loads
γ_F	load effect factor for functional loads
γ_m	material resistance factor
γ_{SC}	safety class factor
ν	Poisson's ratio
ρ_{int}	internal fluid density
ρ_{water}	water density
Δ	offset
β	amplification factor
icp	current profile index
x_{con}	x coordinate of the connection
y_{con}	y coordinate of the connection
HP	horizontal projection

TABLE OF CONTENTS

1 INTRODUCTION

Risers, which are key elements in offshore production systems, along with other technological innovations, have evolved and enabled the production of oil and gas in deepwater fields. In such environments, riser design is complicated by some critical parameters: thicker walls are required due to high hydrostatic pressure, which results in heavier riser and higher cost; the currents can lead to vortex-induced-vibrations (VIV); design of complementary components of attachment of the riser to the host vessel may be necessary to accommodate movements of the vessel due to wave action; significant heave motions from host platform leads to fatigue damage (RUSWANDI, 2009).

The failure of these structures may represent serious environmental and safety risks; therefore, it is necessary to establish a high degree of reliability for riser design. Design requirements are addressed in standards and recommended practices, such as the ones from Det Norske Veritas (DNV), the American Petroleum Institute (API) and the American Bureau of Shipping (ABS), which provide general guides to design, construction and installation of risers for offshore applications.

Since riser design is performed in many stages and the traditional methodology is based on trial and error, it is considerably dependent on the designer's experience. Hence, the problem of elaborating a feasible riser for certain scenario may be treated as an optimization problem. Due to the presence of discrete variables (e.g. type of material and thickness), the utilization of gradient based optimization methods (Mathematical Programming) is not suitable.

Therefore, the main objective of this work was the elaboration and implementation of a model for preliminary design of steel catenary risers. Based on the literature review, wall thickness and material of the riser (which can be made up of one or more segments) were defined as the optimization variables. Instead of using a structural analysis software, a simplified model for static analyses of risers was adopted in the optimization model. In a comparison study, the results obtained with the inextensible cable model and Finite Element analysis, demonstrated the adequacy and accuracy of this this simplified analysis model.

For refinement of the model, a surrogate for prediction of the dynamic amplification factor was developed in this work to be utilized in lieu of the dynamic analysis. Given that many individuals are evaluated during an optimization procedure and the number of loading cases that needs to be considered can be large, the choice of the surrogate modelling approach, instead of an automated routine to perform dynamic analysis in a marine analysis software,

proved to be adequate for preliminary design of steel catenary risers.

This work is organized as follows. Initially, risers material and configurations are briefly reviewed, and the main stages of riser design and the technical standards and recommended practices are discussed (Chapter 2). The developed optimization model, including the functioning of the chosen algorithms, the model parameters, variables, objective function, constraints, analyses procedure, and its implementation are detailed in Chapter 3.

In Chapter 4, the procedure of the elaboration of the surrogate for the dynamic amplification factor is detailed. A concise discussion of design of experiments, number of samples, metamodeling techniques, model training and validation is included. The effectiveness of the proposed optimization model is illustrated with some examples in Chapter 5, also demonstrating its flexibility in terms of problem definition. The final remarks and suggestions for future work are included in Chapter 6.

2 RISERS

The exhaustion of the most profitable and easily accessible resources of oil and gas motivated the industry to focus on exploration and development of new reservoirs located offshore in deep water (from 400 to 1500 m water depth) and ultra-deepwater (water depths of more than 1500 m). In order to make production of oil and gas in such deepwater fields profitable and possible, the industry had to look for technological innovation for the facilities used in the different stages of the production, which should be able to stand the high pressures and low temperatures of these hostile environments. For instance, new platforms, drilling technology, risers and pipelines were developed to comply with the requirements imposed by deepwater fields.

2.1 Riser types – materials and configurations

A riser is a "pipe that connects an offshore floating production structure or a drilling rig to a subsea system either for production purposes such as drilling, production, injection and export or for drilling, completion and workover purposes" (TENARIS, 2017). In respect of materials, there are essentially two kinds of risers, namely flexible risers and rigid risers.

Flexible risers are multiple-layer pipes, with alternate plastic and metallic layers with different structural functions. As illustrated on Figure 1, the flexible riser structure typically contains an internal sheath that acts as internal fluid containment barrier, several tensile steel layers and pressure reinforcement layers, and an external layer that acts as external fluid barrier (CHAKRABARTI, 2005). This combination of sheaths with different properties and functions allow this type of riser to be, at the same time, lightweight, resistant and flexible. However, the cost of flexible risers is usually high.

On the other hand, rigid risers are composed of pipe sections of rigid material (steel, titanium, fiber reinforced composites) that are welded together or coupled together by mechanical connectors located on the ends of each pipe section (e.g. threaded connectors, flanged connectors), which make them easier to be fabricated, and, consequently less expensive than flexible risers. A variety of materials can be used in the manufacture of this type of riser, ranging from carbon steel (API 5L – grade B to X70 or superior) to ferritic, austenitic, martensitic or duplex stainless steel (BAI, Y.; BAI, Q., 2005). Other alternatives, such as titanium and composite made of carbon fibers have been considered, but the main disadvantage of these materials is the high cost and complexity in manufacture.

Figure 1. Typical cross section of flexible pipe

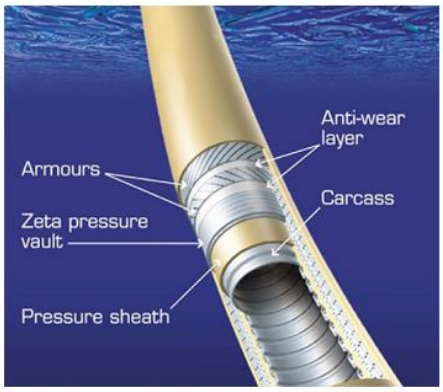

Source: Y. Bai and Q. Bai (2010).

The selection of material grade is a critical stage of the riser design and it should take into consideration the cost, the resistance to corrosion effects, weight requirements and weldability. The choice of the material grade has cost implications on fabrication, installation and operation of the riser. The resistance and cost of fabrication are higher for higher grade steels. However, selecting a higher grade steel may allow a reduction of riser wall thickness, leading to a reduction of weight and tension, and consequently a reduction in riser fabrication cost.

For some of the more sophisticated steels, there are some difficulties in welding the pipe sections, which can delay the installation process and increase the cost of installation of risers made of higher grade steel when compared to lower grade steel riser. Furthermore, depending on the fluid that is going to be conveyed, the riser can be subjected to erosion and corrosion, and the adequate material should be selected in order to assure that such problems do not affect the operation of the riser (BAI, Y.; BAI, Q., 2005).

Risers are one of the most complex aspects of a deepwater production system and they can be installed in different configurations, which range from free catenary to configurations that include floating elements (Figure 2). Riser configuration design is performed according to production requirements and site-specific environmental conditions, such as water depth, host vessel motion characteristics, number and type of risers and mooring layout and environmental data.

In the lazy-wave and steep-wave configurations buoyancy modules are added along a section of the riser, while in lazy-S and steep-S configurations the lateral movement is limited by the utilization of a subsea buoy fixed to a structure at the seabed or positioned by chains (Figure 3). Because of the complexity in the installation, lazy-S and steep-S configurations are usually considered only when catenary and wave configurations are not suitable for the

particular field (LEFFLER; PATTAROZZI; STERLING, 2003).

Figure 2. Riser systems overview

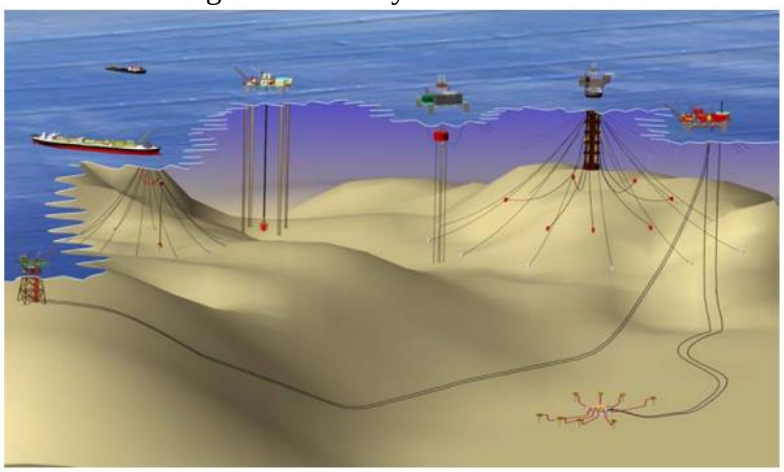

Source: Y. Bai and Q. Bai (2010).

Figure 3. Riser configurations with buoyancy modules.

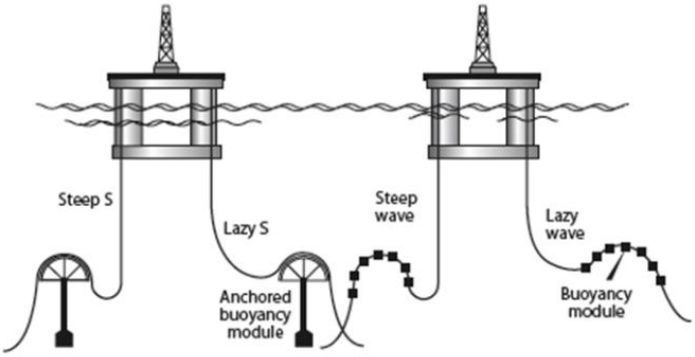

Source: Leffler, Pattarozzi and Sterling (2003).

A buoyant free standing riser is a type of hybrid riser that has a vertical section of rigid metal riser connected to a subsea buoy below wave action zone and a flexible line that interconnects the rigid section and the host platform (Figure 4). This characteristic allows this type of riser to accommodate relative motion between floating structure and rigid riser. Free Standing Hybrid Risers (FSHR) are also relatively insensitive to motion induced fatigue (RUSWANDI, 2009).

Free hanging catenary configuration, in which the riser is fixed at the top end to a vessel and extends freely to the soil (Figure 5), is the simplest and easiest configuration to install and maintain. Steel Catenary Risers (SCRs) are cost-effective alternatives for production of oil and gas and water injection lines on deepwater fields, where flexible risers are not feasible due to economic and technical limitations (BAI, Y.; BAI, Q., 2010). Despite these advantages, SCRs are highly sensitive to environmental loading (due to waves and currents) which results in

fatigue issues in the touchdown zone (TDZ).

Figure 4. Buoyant free standing riser

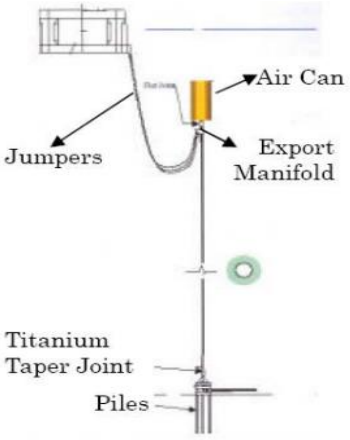

Source: Ruswandi (2009).

Figure 5. Free hanging catenary riser

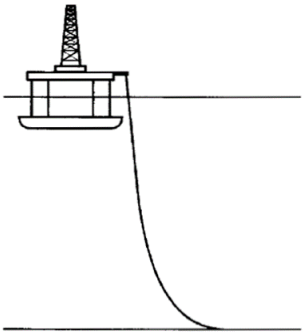

Source: API (1998).

2.2 Design aspects

Given its fundamental functions during all phases of field development (from drilling to production) risers represent key elements in offshore production systems. As can be seen on Figure 6, these structures, along with flowlines, represent 12% of capital expenditures (CAPEX) of subsea development project in deepwater fields (BAI, Y.; BAI, Q., 2010). Moreover, risers are key elements in providing safety. In case of failure of these structures, oil spillage and pollution may occur and lives may be endangered (such as in the accident of Ekofisk Alpha platform in 1975 in which riser rupture occurred (VINNEM, 2007)). Therefore, it is necessary to establish a high degree of reliability for riser design.

Figure 6. Deep water subsea CAPEX

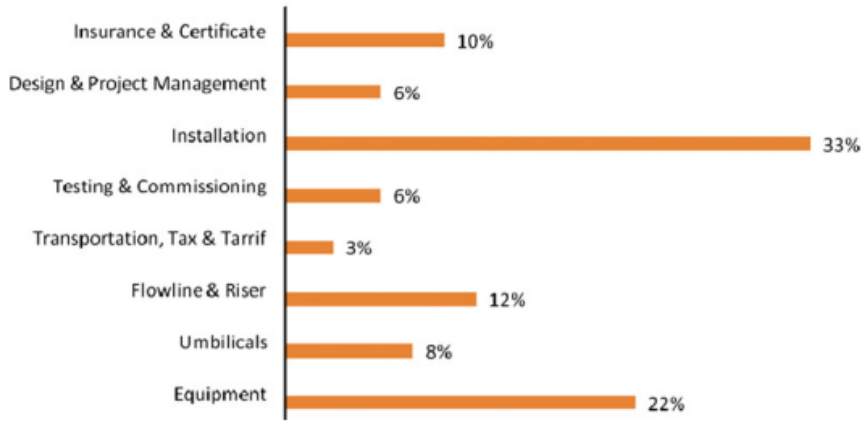

Source: Y. Bai and Q. Bai (2010).

Riser design is performed in many stages, which are summarized in Figure 8. Initially, all the data and conditions for the design of a riser system are specified for the setup of the design basis. Applied codes and standards, design criteria, environmental conditions, design loads and safety factors are defined in this document. A design criterion is used to verify if the designed riser is capable of withstanding all loads anticipated over its specified design life.

In a preliminary front-end engineering design (FEED) phase, riser host layout, location, spacing and azimuth are defined. Then, general sizing of the riser is conducted. Internal diameter sizing is a complex stage and it is a function of the production characteristics of each well, such as flow rate, fluid composition and pressure (TANAKA, 2009). Riser wall thickness sizing is performed based on checks for burst, collapse and combined loads criteria, in accordance with technical standards. For SCRs in deepwater fields, thicker walls are required due to high hydrostatic pressure, which results in heavier riser and higher cost.

Material selection will be influenced by reservoir properties (e.g. pressure and temperature), fluid characteristics (e.g. corrosive fluids), weldability, weight requirements, as mentioned before. The characteristic of high-pressure high-temperature (HPHT) wells may result in de-rating of material steel strength and care has to be taken when selecting the material for such cases.

The loads to be considered in the design of riser systems include pressure loads, functional loads, environmental loads and accidental loads. The pressure loads are due to the combined effect of hydrostatic internal and external pressures. Functional loads are the ones that occur as a consequence of the physical existence of the system and its operation. These include weight and buoyancy of the riser and weight of internal fluid. The environmental loads are imposed directly or indirectly by the ocean environment (waves and currents). The current,

which varies in direction and intensity with depth, acts along the entire riser length. Moreover, current and waves have effect over the platform, resulting in shift in its position, which is referred as offset.

Structural analysis are conducted to check the integrity of the riser under all load combinations. First, static analyses are conducted to determine the equilibrium profile of the riser under the combined effects of self-weight, buoyancy and vessel offset. These analyses are derived for near, mean and far locations of the host platform. Results for effective tension, bending moment, von Mises stress and riser configuration are obtained in the static analysis and used in design code checking. Then, dynamic analyses are conducted to account for the effect of waves over the riser.

Both waves and currents are classified in centenary (100 years), decennial (10 years) and annual (1 year) waves/currents, according to their return periods. The environmental condition is more rigorous for waves and currents with higher return period. The loading cases considered in dynamic analyses are combinations of centenary waves and deccenial currents and vice versa. The risers can be analyzed using regular wave approach, frequency domain random wave approach or time domain wave approach (BAI, Y.; BAI, Q., 2005).

The response amplitude operator (RAO) of the floating facility is an important input for the dynamic analysis, since it describes how the floating facilities respond to the action of the waves. The RAOs depend on the characteristics of the floating facility (e.g. tension leg platforms and semisubmersibles have different sensitivities to waves). Floaters have six degree of freedom: surge, sway, heave, roll, pitch and yaw, as shown in Figure 7 (KONGSBERG, 2017).

Figure 7. Floater motions

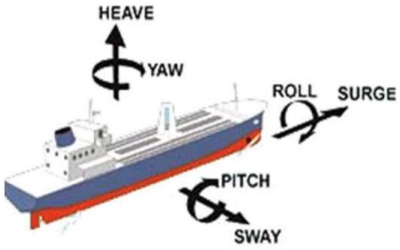

Source: Kongsberg (2017).

Fatigue damage occurs under the action of cyclic loads that happen during fabrication, installation and operation phases, due to collisions, temperature and pressure variations, internal fluid slugging effects, but most importantly because of the action of waves,

currents, winds and floater motions (DNV, 2010b). The fatigue life is defined as the number of stress cycles at a particular magnitude required to cause fatigue failure (DNV, 2011) but is commonly expressed in number of years based on the number of occurrence of the stress cycles per year. Traditionally, SCRs are designed for 25 years or more with a safety factor of 10 to cover all the uncertainties (QUEÁU, 2015).

The general procedure for deterministic fatigue analysis reported in DNV RP-C203 (2011) is summarized as follows. First, the entire wave scatter diagram is divided into representative blocks with one associated sea state per block that constitutes the loading and represents all the sea states within this block. The stress range, generated under the action of a sea state, is used along with a S-N curve to determine the number of cycles that would lead to failure under this loading condition and the damage for each sea state is calculated. This procedure is repeated for every selected sea state for the blocks of the wave scatter diagram and then the individual damages are accumulated using the Palmgren-Miner rule to obtain the total damage ratio. Finally, the fatigue life of the riser is calculated as the inverse of the total damage ratio.

Then, interference and clashing analysis is performed to evaluate the potential interference between: different production risers, production riser and drilling riser, riser and mooring lines, riser and umbilicals, riser and offshore installation, riser and any other obstructions. Local analyses are to be conducted in order to check if clashing involving risers may occur and to ensure the integrity of the structures if it occurs (ABS, 2014).

The next step in the riser design comprises an installation analysis. The pipes for steel risers usually arrives in 40-foot (12.2 meters) sections that are butt-welded together or mechanically coupled to form the line and installed by pipeline laying vessels that follow one of the following installation methods: S-lay, J-lay, reel-lay or tow-in (LEFFLER; PATTAROZZI; STERLING, 2003). The installation analysis is conducted to determine limiting conditions for installation procedures and takes into consideration issues such as load capacity and positioning capacity of installation vessel; interference between the riser in installation and other already-installed risers, mooring lines and umbilicals (ABS, 2014).

Finally, design of complementary components of the subsea riser system, such as connector, VIV suppressors, cathodic protection system, is performed.

Figure 8. Riser Design Flowchart

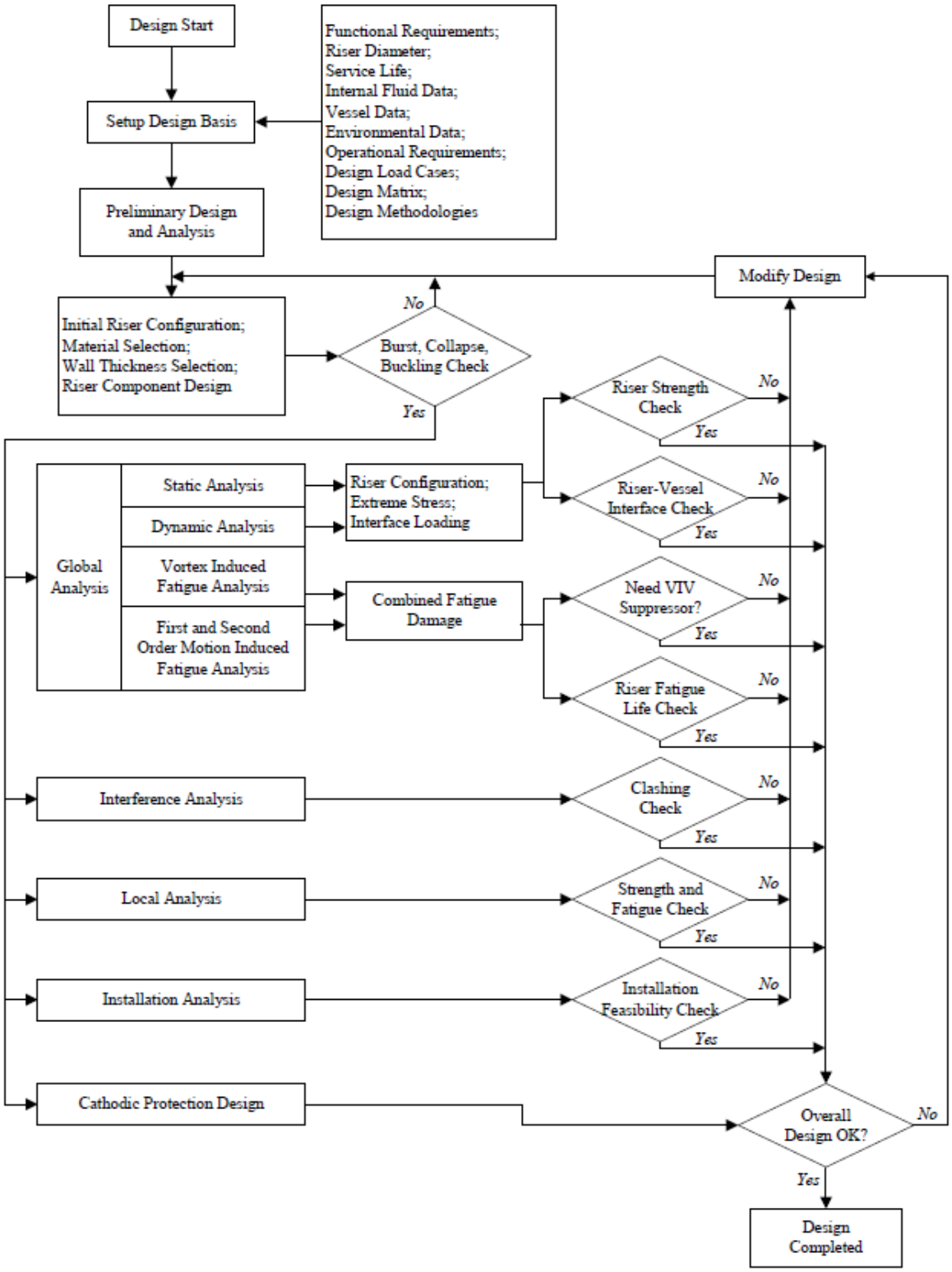

Source: ABS (2014).

2.3 Design codes

A riser shall be designed to answer the specific needs of a project in accordance with technical standards. The most renowned standards and recommended practices for riser design were elaborated by the American Society of Mechanical Engineers (ASME), Det Norske Veritas (e.g. DNV-OS-F101, DNV-OS-F202, DNV-RP-F204), the International Standardization Organisation (ISO) or the American Petroleum Institute (e.g. API 5L, API RP 2RD) (FROUFE, 2006). These standards are referenced throughout this work.

Two design methods that may be applied in riser design are: Working Stress Design (WSD) and Load and Resistance Factor Design (LFRD). The main difference between these methodologies is that the WSD considers a central safety factor for each limit state to account for uncertainties originated from different causes, while the LFRD separates the influence of uncertainties by means of partial safety factors. Then, the WSD is considered as a more conservative design method, while the LFRD allows a more flexible design with uniform safety level (DNV, 2010a).

This work follows the standards and recommended practices of DNV, which will be discussed herein. According to DNV-OS-F201, the limit states are classified as:

- Serviceability Limit State (SLS) requires that the riser must be able to remain in service and operate properly when subjected to operational loads;

- Ultimate Limit State (ULS) requires that the riser must remain intact and avoid rupture, but not necessary be able to operate;

- Accidental Limit State (ALS) requires that the riser must remain intact and avoid rupture when subjected to accidental loads;

- Fatigue Limit State (FLS) requires that the riser must remain fit to function during its service life due to accumulated excessive fatigue crack growth or damage under cyclic loading. Three major issues that can cause fatigue damage include first order wave loading and associated floater motion, second order floater motion and VIVs due to current.

In ULS, the riser shall be designed against bursting, buckling and combined loading criteria. To avoid bursting (rupture of the pipe wall due to internal overpressure), riser shall be designed to satisfy the following condition at all cross sections:

$$P_{li} - P_e \leq \frac{P_b}{\gamma_m \gamma_{SC}} \tag{1}$$

where P_{li} is the local incidental pressure, P_e is the external pressure, γ_m is the material resistance factor that accounts for material and resistance uncertainties (Table 1), γ_{SC} is the safety class factor (Table 2), P_b is the burst resistance given by:

$$P_b = \frac{2}{\sqrt{3}} \frac{2t}{D-t} \min\left(f_y, \frac{f_u}{1.15} \right) \quad (2)$$

where t is the riser wall thickness, D is the riser outer diameter, f_y is the yield strength given by:

$$f_y = (SMYS - f_{y,temp}) \cdot \alpha_U \quad (3)$$

where $SMYS$ is the specified minimum yield stress at room temperature based on the engineering stress-strain curve, $f_{y,temp}$ is the temperature de-rating factor for the yield stress and α_U is the material strength factor (Table 4). The f_u is the tensile strength given by:

$$f_u = (SMTS - f_{u,temp}) \cdot \alpha_U \quad (4)$$

where $SMTS$ specified minimum tensile strength at room temperature based on the engineering stress-strain curve and $f_{u,temp}$ is the temperature de-rating factor for the tensile strength. Values for the temperature derating factors for yield stress and tensile strength can be found on DNV-OS-F201 (2010), accordingly to riser material and temperature of operation.

The local incidental pressure can be calculated at each riser cross section as:

$$P_{li} = 1.1 \cdot P_d + \rho_{\text{int}} \cdot g \cdot h \quad (5)$$

where P_d is the design pressure (maximum surface pressure during normal operations), ρ_{int} is the density of the internal fluid, g is the gravity acceleration, and h is the hydrostatic column at the specified riser cross section.

Table 1. Material resistance factor

	γ_m
ULS, ALS	1.15
SLS, FLS	1.00

Source: adapted from DNV (2010a).

Table 2. Safety class resistance factor

	γ_{SC}
Low	1.04
Normal	1.14
High	1.26

Source: adapted from DNV (2010a).

Table 3. Classification of safety classes

Safety class	Definition
Low	Where failure implies low risk of human injury and minor environmental and economic consequences.
Normal	For conditions where failure implies risk of human injury, significant environmental pollution or very high economic or political consequences.
High	For operating conditions where failure implies high risk of human injury, significant environmental pollution or very high economic or political consequences.

Source: adapted from DNV (2010a).

Table 4. Material strength factor

	α_U
Normal	0.96
Supplementary requirement	1.00

Source: adapted from DNV (2010a).

To avoid buckling (rupture of the pipe wall due to external overpressure), riser shall be designed to satisfy the following condition at all cross sections:

$$P_e - P_{\min} \le \frac{P_{\Pr}}{\gamma_c \gamma_m \gamma_{SC}} \tag{6}$$

where P_{min} is a minimum internal pressure, P_{Pr} is the resistance against buckling propagation, γ_c is a factor that assumes the value of 1.0 if no buckle propagation is allowed. The resistance against buckling propagation P_{Pr} is given by:

$$P_{\Pr} = 35 f_y \alpha_{fab} \left(\frac{t}{D} \right)^{25} \tag{7}$$

where α_{fab} is a fabrication factor that assumes the value of 0.85 in the worst scenario. If the pipe design is sufficient to meet the above propagation criterion, the system hoop buckling (collapse) criterion is also met.

To guarantee riser integrity under combined loading, the following conditions shall be respected in case of net internal overpressure and net external overpressure, respectively:

$$\{\gamma_{SC}\gamma_m\} \left\{ \frac{|M_d|}{M_k} \sqrt{1 - \left(\frac{p_{ld} - p_e}{p_b} \right)^2} + \left(\frac{T_{ed}}{T_k} \right)^2 \right\} + \left(\frac{p_{ld} - p_e}{p_b} \right)^2 \le 1 \tag{8}$$

$$\{\gamma_{SC}\gamma_m\}^2 \left\{ \left(\frac{|M_d|}{M_k} \right) + \left(\frac{T_{ed}}{T_k} \right)^2 \right\}^2 + \{\gamma_{SC}\gamma_m\}^2 \left(\frac{p_e - p_{\min}}{p_c} \right)^2 \le 1 \tag{9}$$

where T_{ed} is the design effective tension, T_k is the plastic axial force resistance, M_d is the design bending moment, M_k is the plastic bending moment resistance, P_{ld} is the local internal design pressure and P_c is the hoop buckling resistance.

The plastic axial force resistance T_k is given by:

$$T_k = f_y \alpha_c \pi (D-t)t \tag{10}$$

and the plastic bending moment resistance M_k is given by

$$M_k = f_y \alpha_c (D-t)^2 t \tag{11}$$

where α_c is a parameter accounting for strain hardening and wall thinning given by:

$$\alpha_c = (1-\theta) + \theta \frac{f_u}{f_y} \tag{12}$$

where

$$\theta = \begin{cases} (0.4 + q_h) & \text{for } \frac{D}{t} < 15 \\ \frac{(0.4 + q_h)\left(60 - \frac{D}{t}\right)}{45} & \text{for } 15 < \frac{D}{t} < 60 \\ 0 & \text{for } \frac{D}{t} > 60 \end{cases}$$

$$q_h = \begin{cases} \frac{p_{ld} - p_e}{p_b} \frac{2}{\sqrt{3}} & \text{for } p_{ld} > p_e \\ 0 & \text{else} \end{cases}$$

The design effective tension T_{ed} is given by:

$$T_{ed} = \gamma_F T_{eF} + \gamma_E T_{eE} + \gamma_A T_{eA} \tag{13}$$

where γ_F, γ_E, γ_A are the load effect factors for functional, environmental and accidental loads respectively (Table 5), T_{eF}, T_{eE}, T_{eA} are the effective tension from functional, environmental and accidental loads, respectively.

The design bending moment M_d is given by:

$$M_d = \gamma_F M_F + \gamma_E M_E + \gamma_A M_A \tag{14}$$

where M_F, M_E, M_A are the bending moment from functional, environmental and accidental loads, respectively.

Table 5. Load effect factor

Limit state	γ_F	γ_E	γ_A
ULS	1.1	1.3	NA
FLS	1.0	1.0	NA
SLS, ALS	1.0	1.0	1.0

Source: adapted from DNV (2010a).

The hoop buckling resistance P_c is calculated from:

$$(p_c - p_{el})(p_c^2 - p_p^2) = p_c\, p_{el}\, p_p\, f_0\, \frac{D}{t} \tag{15}$$

where f_o is the ovality, P_p is the plastic collapse pressure and P_{el} is the elastic collapse pressure. This equation has the following analytical solution (DNV, 2013):

$$p_c = y - \frac{1}{3}b \tag{16}$$

where

$$b = -p_{el}$$

$$c = -\left(p_p^2 + p_{el}\, p_p\, f_0\, \frac{D}{t} \right)$$

$$d = p_{el}\, p_p^2$$

$$u = \frac{1}{3}\left(-\frac{1}{3}b^2 + c \right)$$

$$v = \frac{1}{2}\left(\frac{2}{27}b^3 - \frac{1}{3}bc + d \right)$$

$$\phi = \cos^{-1}\left(\frac{-v}{\sqrt{-u^3}} \right)$$

$$y = -2\sqrt{-u}\cos\left(\frac{\phi}{3} + \frac{60\pi}{180} \right)$$

The plastic collapse pressure P_p is given by:

$$p_p = 2\frac{t}{D}\, f_y \alpha_{fab} \tag{17}$$

The elastic collapse pressure P_{el} is given by:

$$p_{el} = \frac{2E\left(\frac{t}{D} \right)^3}{1 - \nu^2} \tag{18}$$

where E is the Young's Modulus and ν is the Poisson's ratio.

3 RISER OPTIMIZATION

The utilization of optimization procedures in the field of Petroleum Engineering has been increasing recently, such as in the optimization of production operations (WANG, 2003; WANG; FENG; HAYNES, 2015), optimization of waterflooding management (HOROWITZ; AFONSO; MENDOÇA, 2013), optimization of artificial lift systems such as electric submersible pumps (ADHAV; SAMAD; KENYERY, 2015), riser optimization (LARSEN; HANSON, 1999; PINA *et al.*, 2011; VIEIRA; LIMA; JACOB, 2012; SILVA *et al.*, 2013; TANAKA; MARTINS, 2007; DE ANDRADE *et al.*, 2010), and other problems.

The objective of an optimization procedure is to find not only a satisfactory solution, but an optimal solution that minimizes a cost function and respects all safety criteria and fabrication constraints. The optimization algorithms can be deterministic (such as Linear Programming and Sequential Quadratic Programming) or random (such as Genetic Algorithm, Particle Swarm Optimization, and Simulated Annealing). Deterministic algorithms require continuous and differentiable objective and constraint functions in the search domain. However, this is not the case for most of the engineering applications. For these cases, algorithms such as Genetic Algorithm (GA) and Particle Swarm Optimization (PSO), which are included in the class of bio-inspired algorithms, may be utilized.

Larsen and Hanson (1999) developed a methodology for optimization of steel catenary risers considering only static scenarios. The design variables chosen by the authors were the length and thickness of riser segments and the horizontal distance from lower to upper end of the riser at far position. Since the variables were considered as continuous, a Sequential Quadratic Programming (SQP) scheme was adopted. For the global riser analysis, initially an approximated solution is found by catenary theory, and this solution is then applied as starting point for a finite element method. The objective was to minimize the riser total cost and restrictions related to design variables bounds, global geometry (sum of the segments must exceed the length of a straight line between the ends of the riser), minimum riser length in contact with the seafloor, maximum equivalent stress and local buckling capacity are considered. The numerical examples presented by the authors demonstrated the usefulness of optimization tools for the design of catenary risers.

With the objective of defining the best values and variation behavior of the set of parameters of the PSO algorithm, Pina *et al.* (2011) developed a methodology for the optimization of steel lazy-wave riser connected to platform by a flex-joint. The riser analysis is performed using a catenary solver. The design variables are the lengths of top riser segment,

riser segment with distributed floater, lower riser segment and buoy length, buoy diameter and buoy spacing. The objective function is the total cost of the riser. Restrictions of maximum equivalent von Mises stress, maximum angle between riser axis and the vertical direction at the connection with the platform, maximum "built in" angle (dictated by the design of the flex joint), maximum tension at riser top and minimum tension at the riser bottom are considered. For a numerical example considering only static load cases, PSO and some of its variants were tested. As the result of the employed methodology, the authors were able to tailor a PSO algorithm for the design of steel lazy-wave risers and developed a user-friendly optimization tool.

In order to perform a more extensive comparison between different optimization strategies based on evolutionary concepts, Vieira, Lima and Jacob (2012) adopted the same model developed by Pina *et al.* (2011), but tested other algorithms, such as GA, Genetic Algorithm with Adaptive Fuzzy Fitness Granulation (AFFG) and Artificial Immune System (AIS). As exposed by the authors, the main purpose of the AFFG technique is to reduce the number of fitness evaluations during the optimization process with the GA, replacing expensive exact evaluations by an approximation model. On the other hand, AIS follows ideas taken from immunology to develop computational systems capable of performing different tasks such as optimization, data analysis and machine learning. In AIS, the antibodies are the candidate solutions of the problem, and their quality is called affinity. On the example illustrated by the authors, a better performance was obtained with the AIS variants, closely followed by the PSO.

Silva *et al.* (2013) proposed a methodology for the optimization of composite catenary risers subjected to multiple load cases. The design variables considered in the model were the thickness and fiber orientation of each layer of the composite. The layup was considered constant along the riser, since considering different properties along the riser length would lead to increased computational cost. The riser analysis was performed in global and local levels. For the global analysis, an analytical catenary solver was used. For the local analysis, the classical lamination theory was adopted. The objective was to minimize the cross sectional area of the riser. To verify the strength of the metallic liner, von Mises failure criterion was employed, while for the strength verification of the composite layers, maximum stress or Tsai-Wu failure criteria was adopted. The methodology was implemented in MATLAB (MATHWORKS, 2010) and three different optimization algorithms were considered: SQP, Penalty Function (PF) approach and GA. From the tested numerical examples, the authors concluded that the SQP for continuous variables was the most efficient, while GA was the most time consuming, but GA solutions had greater diversity, presenting more choices to the designer.

Tanaka and Martins (2007) developed a model for optimization of steel risers for free-hanging catenary and lazy wave configurations considering dynamic loads. For this purpose, it was considered that the riser had three segments and the lengths of these segments were the design variables. The floater thickness of the second segment was also a design variable. Materials, inner and outer diameters of the segments were considered as given. The riser analysis for static problem was based in the direct integration of the differential equations which govern the behavior of the riser without bending stiffness ($EI = 0$), via a Runge-Kutta method. For dynamic analysis, a finite element model was used. Since simulations of dynamic conditions can slow down the optimization process, only one extreme dynamic condition was considered on the examples illustrated by the authors. The objective function chosen by the authors was the maximum stress amplitude of the dynamic problem solution. This choice of objective function was motivated by the fact that performing actual fatigue calculation during the optimization would be computationally too costly. Then, by minimizing such stress, the authors expect that the fatigue life would be maximized. Based on standard design practices, constraints on minimum tension along the riser, minimum curvature radius and maximum stress were defined. The optimization algorithm chosen by the authors was GA.

An optimization procedure for steel lazy wave riser configuration for spread moored FPSOs was developed by De Andrade *et al.* (2010) considering riser segments lengths, top angle and buoy diameter, spacing and length as design variables. Before proceeding to the optimization, the authors conducted extensive extreme load analysis of the risers for all the involved load cases and identified the most critical riser configuration and the most critical environmental condition associated. The riser analysis was performed with the software ANFLEX (PETROBRAS, 2001). A multiobjective formulation was adopted by the authors with the objective of minimizing floater volume, tension force at the riser top and code criteria by DNV. The constraints applied were related to geometric limits and criteria defined in DNV-OS-F201. The optimization was carried out using the software modeFRONTIER (ESTECO, 2009) and the chosen algorithm was the Non-dominated Sorting Genetic Algorithm II (NSGA-II). It is important to note that the optimization process was performed primarily to search for configurations that met the extreme load analysis criteria, while the VIV and installation analyses were performed outside the optimization process. The installation analysis was performed focusing on identifying the maximum tension forces, maximum stresses and verification of compression during the riser installation procedure. The VIV analysis was performed using Shear7 (VANDIVER, 2007) to identify fatigue damage at the touch down point (TDP) and to determine the extension of the riser that would need VIV suppressors. By adopting

this methodology, the authors confirmed that such optimization technique reduces the effort of generating preliminary steel lazy wave riser configurations that meet design code criteria.

In this work, an optimization model for SCRs was developed. This chapter will discuss the details of the developed optimization model, including the functioning of GA and PSO, and the model parameters, variables, objective function, constraints and analyses procedure, and its implementation.

3.1 Optimization algorithms

3.1.1 Genetic Algorithms

The Genetic Algorithms, first studied by John Holland in the 1970's, is based on the ideas of natural selection proposed by Darwin and genetic heritance proposed by Mendel (ARORA, 2012). According to Darwin's theory, the individuals that are most adapted to the environment have greater chances of transmitting their genetic characteristics to the next generations, while the least adapted individuals tend to disappear.

In this optimization algorithm, individuals represent possible solutions of the optimization problem, and these are subjected to natural evolution, genetic recombination and mutation, which will be discussed later. In the context of riser optimization, it means that each individual represents a set of data that defines certain riser design in the domain of the problem solutions, and this data is encoded in the individual's chromosomes. Furthermore, the set of individuals, which evolves throughout the generations, corresponds to the population.

In respect to riser optimization, the determination of the quality of a possible solution, which represents the individual fitness, requires the execution of an analysis procedure for the determination of the riser response and the calculation of the constraints. The individuals with higher fitness – corresponding to the best solutions of the optimization problem – are able to pass their genetic material (the encoded riser data) to the next generations, while the individuals with lower fitness – corresponding to improbable riser designs – tend to disappear.

In the functioning of the algorithm (summarized in Figure 9), the random generation of a population of individuals is the first step. In this step, an important parameter is the population size, which defines the number of individuals that will be evaluated in each generation. Although an increase in the population leads to a better exploration of the search space, the computational cost will increase, since more individuals (i.e. designs) will be analyzed.

Then, the fitness of each individual of the population is calculated based on the penalized objective function of the problem. In a minimization problem, as is the case in this work, individuals with lower values for the objective function have higher fitness and are assigned greater probabilities of selection for crossover (ROCHA, 2013). With the calculated fitness, pairs of individuals are randomly selected for crossover. There are different mechanisms for the selection of these pairs, such as ranking, roulette and tournament (ARORA, 2012).

The crossover involves the breakdown of the chromosome in certain points and the recombination of the parts. This genetic operator, which is responsible for the convergence of the method, is applied to the pairs of individuals (parents) and generates two new individuals (sons) with the characteristics of both parents. In a mechanism referred as elitism, the best individuals of a previous generation are copied to the next generation. This algorithm feature guarantees that the best solutions do not worse from one generation to another (BARROSO, 2015).

Figure 9. Genetic algorithm functioning diagram

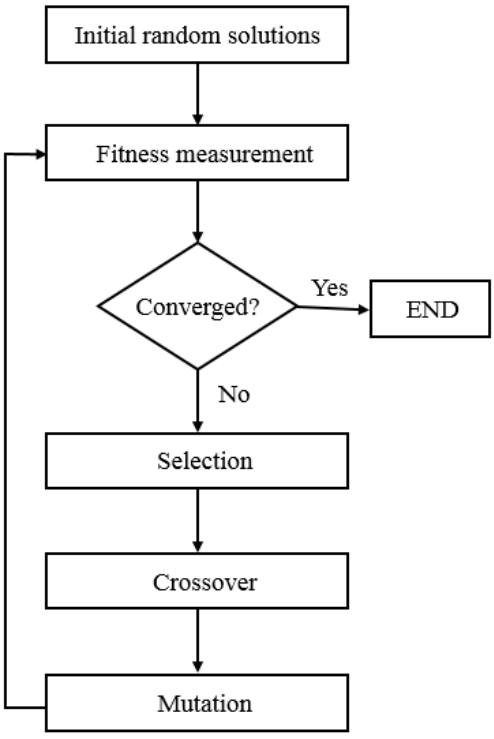

Source: author.

In addition, mutation, which increases the diversity of the population throughout the generations, can occur with certain probability. This is an important operation for the avoidance of premature convergence to a local minimum, and thus increases the chance of

finding the global minimum of the problem. These operations are repeated until a stop criterion (e.g. maximum number of generations, maximum number of generations without improvement of the penalized objective function) is met.

3.1.2 Particle Swarm Optimization

The Particle Swarm Optimization, proposed by Kennedy and Eberhardt (1995), mimics the social behavior of animals, such as flock of birds and schools of fishes, in the search for food. As in GA, the PSO involves a population of individuals or particles, which represent potential solutions of the optimization problem, but in this case the search of the particle swarm is guided by social interactions (VIEIRA, 2009). This means that each particle moves in the search space cooperating and competing with the other particles through successive iterations (BRATTON, 2007). In other words, each particle learns from its own previous experiences and from the swarm experience, evaluating its performance, comparing it to the other particles performance, and then mimicking only the more successful particles.

Firstly, a set of particles is randomly generated. Each particle is represented by a vector $\mathbf{x}$, with dimension equal to the number of design variables. Each particle $\mathbf{x}^i$ has an associated velocity vector $\mathbf{v}^i$. The fitness function is evaluated for each of the particles and it is compared to the best fitness value for the particle from all previous iterations, and the correspondent position $\mathbf{x}^i_p$ is stored. The particle in the neighborhood with the best success is identified and its correspondent position $\mathbf{x}^i_g$ is updated.

The particles position and velocity are iteratively updated by the following expressions, until a stop criterion is met.

$$\mathbf{x}^i = \mathbf{x}^i + \mathbf{v}^i \tag{19}$$

$$\mathbf{v}^i = w\mathbf{v}^i + r_1 c_1(\mathbf{x}^i_p - \mathbf{x}^i) + r_2 c_2(\mathbf{x}^i_g - \mathbf{x}^i) \tag{20}$$

where w is the particle inertia constant, c_1 is the cognitive factor, c_2 is the social factor, r_1 e r_2 are random numbers uniformly distributed in the interval [0, 1], x^i_p is the best position found by the particle until the present iteration and x^i_g is the best position found by neighboring particles. It is important to mention that the particle position is represented by a matrix of integers, while the particle's velocity is represented by a matrix of real numbers and, for the update of the particle position, rounding to the nearest integer is considered.

Since the development of the PSO by Kennedy and Eberhardt (1995), many other variations of the method have been proposed, such as the introduction of a term related to the passive congregation force (which refers to an attraction of an individual to other group members but where there is no display of social behavior) (HE *et. al*, 2004; ALBRECHT, 2005), linear and non-linear variation of the inertia coefficient (EBERHARDT; SHI, 2000; CHATTERJEE; SIARRY, 2006), linear variation of the aggregation and congregation coefficients (RATNAWEERA *et al.*, 2004; PINA *et al.*, 2011)

In the initial version of PSO (KENNEDY; EBERHARDT, 1995), the neighborhood was defined as the whole swarm, referred as Global Topology. This topology generally leads to a fast convergence, but makes the algorithm highly susceptible to premature convergence to non-optimal solutions (BARROSO; PARENTE JR.; MELO, 2017). Later, in order to solve this problem of premature convergence, the interactions between a particle and the neighboring particles and the influence of the topology on the particles' learning were studied and other swarm topologies (e.g. Ring Topology, Square Topology) were proposed (Figure 10).

Figure 10. Swarm topologies

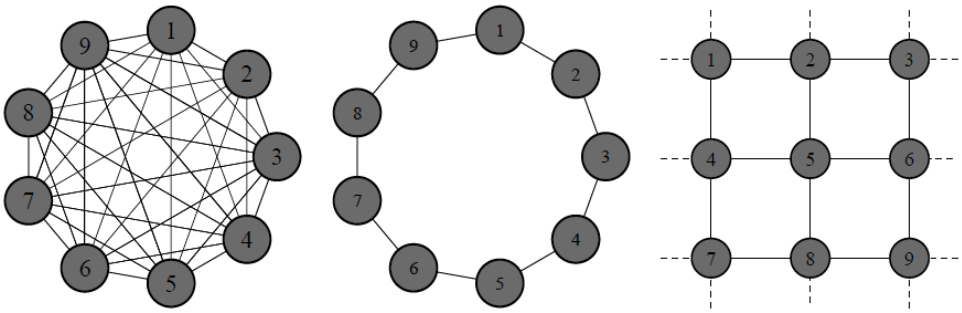

a) Global b) Ring c) Square

Source: Barroso, Parente Jr. and Cartaxo (2017)

3.2 Definition of the optimization problem

As previously discussed, the design of a riser with acceptable structural performance for a given scenario can be exhaustive, since many parameters and safety aspects are involved. Therefore, the main objective of this work was to develop and implement a model for the optimization of SCRs subjected to multiple load cases. The model details will be discussed in the following subsections.

3.2.1 Model parameters

The model parameters involve all the data that is constant along the optimization process (Table 6). This includes the data that defines the scenario, such as the water depth, the coordinates of the connection, the still water level and the horizontal projection (horizontal distance from lower to upper end of the riser), and the safety factors. Each load case considered in the optimization model is described by a set of data, as presented in Table 7. Also, each current profile is defined by a number of points that correlates depth and current velocity.

The optimization algorithm parameters are defined in a specific input file. For both algorithms, it is necessary to specify the optimization number, the maximum generations, the population size (number of individuals) and the constraint tolerance. For GA, is necessary to specify the selection method (ranking or fitness proportional), the crossover rate, and the mutation probability. If PSO is the optimization algorithm chosen, the input file should include the swarm topology (square, ring or global), the particle inertia, the cognitive factor, the social factor. The structure of this file is described in Appendix A.

Table 6. Model parameters

Parameter	Symbol
Gravity acceleration	g
Water density	ρ_{water}
Still water level	SWL
Connection coordinates	(x_{con}, y_{con})
Horizontal projection	HP
Safety class factor	γ_{SC}
Material resistance factor	γ_m
Buckling propagation factor	γ_c
Material strength factor	α_U
Material fabrication factor	α_{fab}
Temperature derating factor for the yield stress	$f_{y,temp}$
Temperature derating factor for the tensile strength	$f_{u,temp}$

Source: author.

Table 7. Data that define a load case

Parameter	Offset	Internal fluid density	Pressure at riser top	Amplification factor	Load effect factor for functional loads	Load effect factor for environmental loads	Current profile index
Symbol	Δ	ρ_{int}	P_d	β	γ_F	γ_E	icp

Source: author.

3.2.2 Design variables

In the literature review on SCRs optimization models and riser design methodology, the conclusions of the following authors were fundamental to the choice of the design variables of the proposed model. Karunakaran *et al.* (2005) presents the concept of weight optimized SCR, in which a variation in weight along the riser is achieved by the application of different density coatings along the riser length, indicating a remarkable improvement in SCR strength. Chandrasekaran and Jain (2016) argue that weight distribution along riser length profile may also be accomplished by varying the steel wall thickness of the riser. When designing risers for water depths between 3000 m and 4500m, Saglar, Toleman and Thethi (2015), indicated that an advantage could be gained if wall thickness of the top section of the riser was increased (instead of a single specified wall thickness for the entire riser). However, they did not consider this design in their work.

Based on the considerations and findings of the reviewed works, the design variables chosen for the optimization model were the material and thickness of the riser, which can be made up of only one segment or multiple segments. In the implementation, each possible design is represented by a matrix with two rows (the first row represents the material and the second row represents the thickness of the segments) and number of columns equal to the number of riser segments.

An integer encoding is used to represent the discrete variables, where each value assumed by the optimization variables represents the index of a list of discrete values. The possible materials and values for thickness are defined in the input file of the optimization. The structure of this file is described in Appendix A. Table 8 and Table 9 illustrate the encoding for the consideration of nine types of materials (represented in the encoding by numbers 0 to 8) and twenty possible values for wall thickness (represented in the encoding by numbers 0 to 19).

In GA parlance, the codified variables correspond to the genotype of an individual, while the decodified values correspond to its phenotype. The genotype is used by the algorithm operators, while the phenotype is used for the evaluation of the fitness function. For a riser with three segments, the codified variables of a possible design could be, for example:

$$\begin{bmatrix} 6 & 4 & 7 \\ 10 & 8 & 12 \end{bmatrix}$$

which represents a riser in which the first segment is made up of API 5L X65 steel and thickness of 0.030 m, the second segment is made up of API 5L X56 and thickness of 0.025 m and the third segment is made up of API 5L X70 steel and thickness of 0.035 m, as illustrated on Figure

11.

Table 8. Material encoding

Code	Material
0	B
1	X42
2	X46
3	X52
4	X56
5	X60
6	X65
7	X70
8	X80

Source: author.

Table 9. Thickness encoding

Code	Thickness (mm)	Code	Thickness (mm)
0	5,0	10	30,0
1	7,5	11	32,5
2	10,0	12	35,0
3	12,5	13	37,5
4	15,0	14	40,0
5	17,5	15	42,5
6	20,0	16	45,0
7	22,5	17	47,5
8	25,0	18	50,0
9	27,5	19	52,5

Source: author.

The mechanical properties of commercially available steels can be found on technical standards, such as in API Specification 5L (2004). Values for yield stress and tensile strength of the materials on Table 8 are listed on Table 10. These material properties are also specified on the input file of the optimization, along with the material density, Young's Modulus and Poisson's ratio.

Figure 11. Example of encoding for a possible riser design

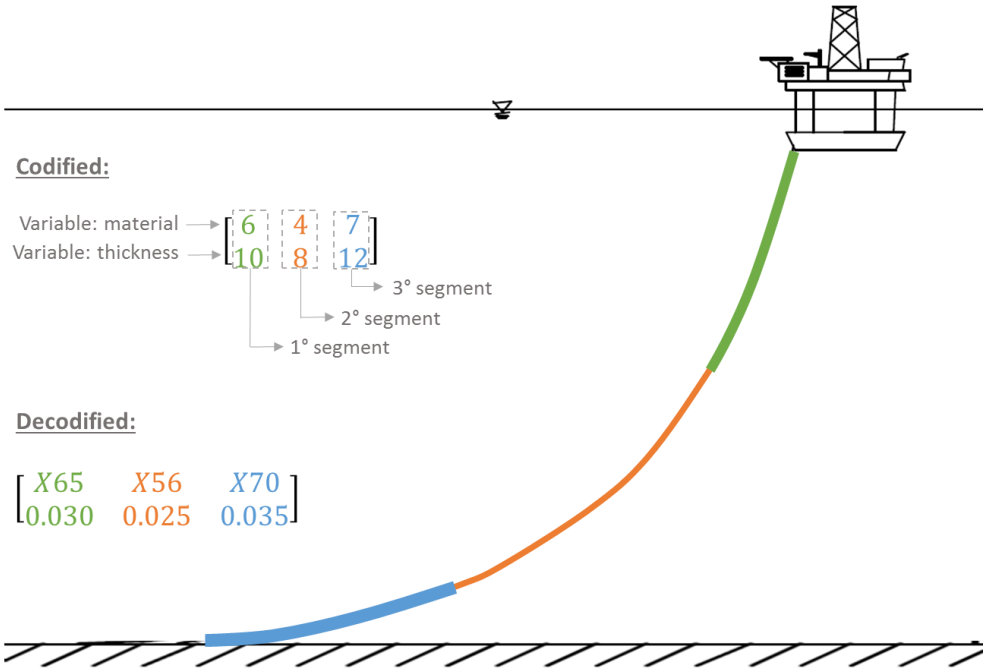

Source: author.

Table 10. Mechanical properties of the materials

Classification	Yield Stress (MPa)	Tensile strength (MPa)
B	241	414
X42	290	414
X46	317	434
X52	359	455
X56	386	490
X60	414	517
X65	448	531
X70	483	565
X80	552	621

Source: author.

3.2.3 Objective function

The chosen objective function was the riser cost, given by

$$f_{obj} = \sum_{i=1}^{n} \pi (R_e^2 - R_i^2) L_i C_i \tag{21}$$

where n is the number of riser segments, R_i is the internal radius of the segment, R_e is the external radius of the segment, L_i is the length of the segment and C_i is the cost (volumetric) of

the material of the segment (defined in the input file of the optimization).

3.2.4 Constraints

The model restrictions follow the verification for the ULS in the normal safety class, as defined in DNV-OS-F201 (2010). Checks for bursting, buckling and combined load are included, according to Eq. (1), (6), (8) and (9). Since the analysis procedure adopted in the optimization model disregards the bending stiffness, the design bending moment (M_d) and plastic bending moment resistance (M_k) terms in Eq. (8) and (9) are null.

Then, the optimization model can be summarized as follows:

find $x = \begin{bmatrix} material_1 & \dots & material_n \\ t_1 & \dots & t_n \end{bmatrix}$

that minimizes $f(x) = \sum_{i=1}^{n} \pi (R_e^2 - R_i^2) LC$

subjected to:

$$g_1(x) = \frac{SF_{req}^{brst}}{SF_n^{brst}} - 1 \le 0, \text{ where } SF_{req}^{brst} = \gamma_m \gamma_{SC} \text{ and } SF_n^{brst} = \frac{P_b}{P_{li} - P_e};$$

$$g_2(x) = \frac{SF_{req}^{bckl}}{SF_n^{bckl}} - 1 \le 0, \text{ where } SF_{req}^{bckl} = \gamma_c \gamma_m \gamma_{SC} \text{ and } SF_n^{bckl} = \frac{P_{\Pr}}{P_e - P_{\min}};$$

$$g_3(x) = \{\gamma_{SC}\gamma_m\} \left\{ \left(\frac{T_{ed}}{T_k} \right)^2 \right\} + \left(\frac{p_{ld} - p_e}{p_b} \right)^2 - 1 \le 0;$$

$$g_4(x) = \{\gamma_{SC}\gamma_m\}^2 \left\{ \left(\frac{T_{ed}}{T_k} \right)^4 \right\} + \{\gamma_{SC}\gamma_m\}^2 \left(\frac{p_e - p_{\min}}{p_c} \right)^2 1 \le 0.$$

3.2.5 Riser analysis

Riser analysis can be carried out by different procedures, ranging from simpler models based on catenary equations to more complex models such as Finite Element Model (FEM). In the proposed methodology, a simplified model for static analyses of risers is used with the objective of determining the geometry and acting forces. This model considers the riser as an inextensible cable subjected to vertical loads (weight and buoyancy), horizontal loads (current) and floater offset. A more detailed description of the model can be found on the work by Alves and Parente Jr. (2016).

With the objective of validating the analysis model, different risers were analyzed using both the mentioned inextensible cable model and FLEXCOM (MCS KENNY, 2013), a structural analysis software package widely used in the offshore oil and gas industry, and the obtained results were compared. For illustration of the efficiency of the adopted analysis model, the comparison for a riser made of API 5L X56 steel with total length of 2520 m, internal radius of 0.125 m, thickness of 0.025 m, installed in a scenario with water depth of 1500 m and horizontal projection of 1732 m, is included.

The model for this riser on FLEXCOM can be seen on Figure 12. A total of 250 elements, numbered from the anchor to the connection, were considered. The load cases considered in this comparison are specified on Table 11 and the current data are detailed on Table 12. For each of the load cases, results for effective tension and geometry were compared. As can be seen on Table 13, the differences for effective tension at the anchor between the inextensible cable model and FLEXCOM are within ±3.5%. Furthermore, the differences for the effective tension at the connection are smaller than ±1%. In addition, a comparison of the computational cost of both procedures was carried-out and the results showed that the inextensible cable model was 16 to 26 times faster than FLEXCOM.

Figure 12. Riser model in FLEXCOM

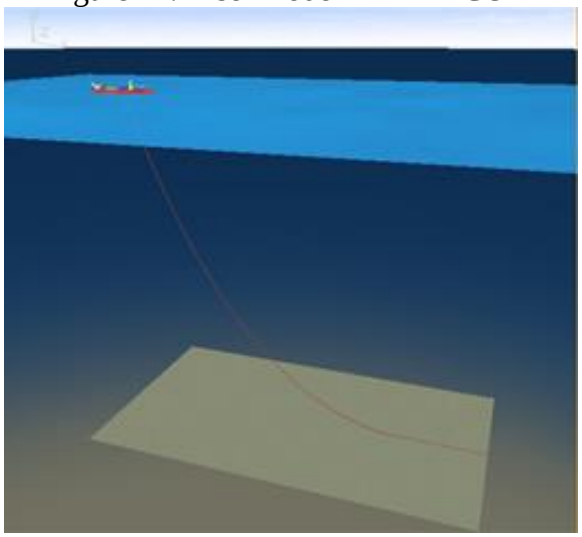

Source: author.

Comparison studies such as the previously mentioned were carried out for other riser models and the obtained differences were in the same range. These studies demonstrated the quickness of the inextensible cable model in comparison with FE analysis. Taking into consideration the accuracy and lower execution time of the inextensible cable model, it can be

concluded that this simplified analysis model is adequate for the proposed optimization model, since many individuals have to be evaluated during the optimization process.

Table 11. Load cases data for comparison of riser analyses results using the inextensible cable model and FLEXCOM

Load case	Internal Fluid	Offset		Current	
		Direction	% SWL	Return period	Direction
1	Oil	near	8.5	-	-
2	Oil	far	8.5	-	-
3	Empty	near	8.5	-	-
4	Empty	far	8.5	-	-
5	Water	near	3.0	-	-
6	Water	far	3.0	-	-
7	Oil	near	8.5	100	E
8	Oil	far	8.5	100	W
9	Empty	near	8.5	100	E
10	Empty	far	8.5	100	W
11	Water	near	3.0	1	E
12	Water	far	3.0	1	W

Source: author.

Table 12. Current data

Depth [m]	Velocity [m/s]			
	CE 1	CE 100	CW 1	CW 100
0	0.85	1.70	0.97	1.79
100	0.76	1.52	0.78	1.44
350	0.70	1.40	0.75	1.39
500	0.46	0.92	0.52	0.96
1000	0.35	0.70	0.36	0.67
1500	0.27	0.54	0.35	0.65

Source: author.

Table 13. Results for effective tension using the inextensible cable model and FLEXCOM

Load case	Effective Tension at Anchor [kN]			Effective Tension at Connection [kN]		
	Flexcom	Cable	Diff.	Flexcom	Cable	Diff.
1	655.0	659.8	0.73%	2718.9	2723.5	0.17%
2	1754.4	1770.0	0.89%	3817.0	3830.0	0.34%
3	456.4	457.0	0.13%	1884.9	1880.0	-0.26%
4	1222.1	1230.0	0.65%	2650.4	2650.0	-0.02%
5	945.7	953.0	0.77%	3113.0	3121.6	0.28%
6	1334.1	1350.0	**1.19%**	3501.3	3510.0	0.25%
7	579.1	595.4	**2.82%**	2642.2	2659.1	0.64%
8	1847.9	1848.5	0.03%	3910.4	3919.2	0.23%
9	379.0	392.4	**3.54%**	1808.1	1820.7	0.70%
10	1315.8	1303.4	-0.94%	2744.0	2732.0	-0.44%
11	952.2	923.4	-**3.02%**	3092.6	3092.0	-0.02%
12	1360.0	1379.3	**1.42%**	3527.1	3547.9	0.59%

Source: author.

3.2.6 Implementation

The proposed model was implemented in *BIOS* (*Bio-inspired Optimization System*), an optimization program written in C++ language according to the principles of Object-Oriented Programming (OOP) at the Laboratório de Mecânica Computacional e Visualização (LMCV) of the Universidade Federal do Ceará (UFC). For the optimization process, the data is defined in two input files: one of the files includes the model parameters; and the other contains the optimization algorithm parameters. More details about these input files are included in Appendix A.

4 SURROGATE FOR DYNAMIC AMPLIFICATION FACTOR

4.1 Surrogate modelling

In many industries (such as in the aerospace, automotive and electronics industries) design problems are slow down by the computational burden incurred by expensive analysis and simulation processes. To address such challenge and to improve overall computation efficiency, surrogate models (also referred as metamodels) have been developed to replace these expensive numerical simulation procedures (WANG; SHAN, 2006).

The objective of a surrogate is to emulate the behavior of the actual expensive numerical procedure (also referred as high fidelity model), by capturing the relationship between the inputs and outputs. Once built, it provides fast analysis tools for exploration of the design space and optimization by using approximations in lieu of the computationally expensive analysis code themselves (SIMPSON *et. al*, 2001).

While the basic idea of the surrogate approach may sound simple, there are many details involved in this technique, including the choice of a design of experiments for data generation, the choice of a model to represent this data and the fitting of the model to the observed data (FORRESTER; SÓBESTER; KEANE, 2008). For each of these steps there are several options, as it will be discussed.

The surrogate modelling process can be summarized as follows (Figure 13): first, the model variables are selected according to preliminary experiments; then, samples are generated according to a sampling plan; next, a surrogate model type is selected and used to build a model of the underlying problem; later, new design points are analyzed and the results are added for upgrade of the surrogate, if necessary (FORRESTER; KEANE, 2009).

The surrogate modelling techniques include Kriging, Artificial Neural Networks (ANN), Radial Basis Functions (RBF), Multivariate Adaptive Regressions Splines (MARS), Support Vector Machine (SVM) (WANG; SHAN, 2006). In the field of Petroleum Engineering, these techniques can been applied to different kinds of problems.

For example, ANNs have been applied for prediction of geomechanical parameters and to assist in wellbore instability studies (OKPO; DOSUNMU; ODAGME, 2016), to generate pseudo-density logs that can be used in reservoir characterization (LONG; CHAI; AMINZADEH, 2016), to predict troubles due to geological and technical factors during drilling of oil and gas wells (LIND; KABIROVA, 2014), for prediction of wax deposition in tubulars (ADEYEMI; SULAIMON, 2012), to predict gas injection rate and oil production rate for wells

under gas lift operations (RANJAN; VERMA; SINGH, 2015), to analysis of spread-mooring configurations for floating production systems (PINA *et al.*, 2016).

Moreover, Kriging has been utilized in design optimization of electric centrifugal pumps (ADHAV; SAMAD; KENYERY, 2015) and for reservoir management optimization (PINTO, 2014), SVM has been used to assist in seismic interpretation (ZHAO *et. al*, 2014) and for prediction of PVT properties of crude oil systems (EL-SEBAKHY *et. al*, 2007), RBF has been applied to optimization of shaped-charge explosives of perforating guns (MCDONALD *et. al*, 2007) and riser design (CHEN *et al.*, 2015).

Figure 13. Surrogate modelling framework

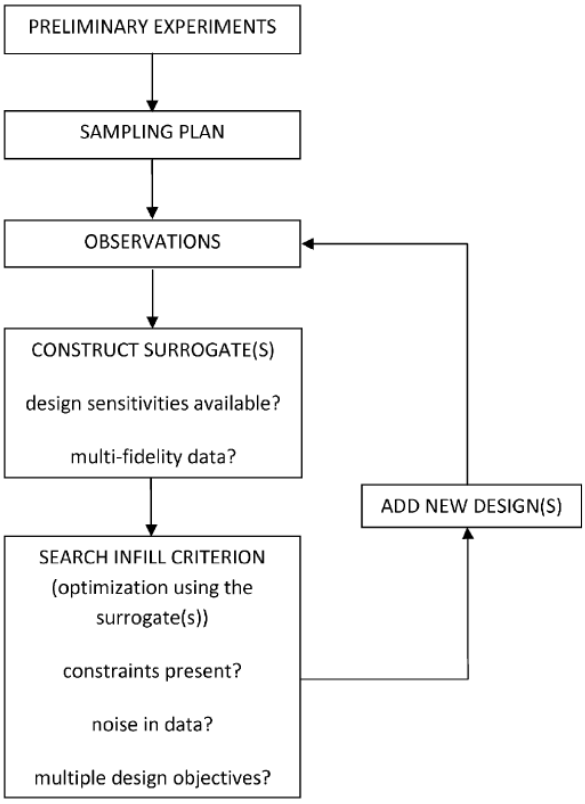

Source: Forrester and Keane (2009).

4.1.1 Surrogate variables and sampling plan

The selection of the variables is the first step in surrogate modelling. A high number of variables may represent a limitation, since the number of samples needed to give reasonably uniform coverage rises exponentially (the so-called curse of dimensionality). While the selection of variables in a familiar design problem may be obvious, in new design problems it

may be necessary to perform screening and sensitivity studies to identify the variables that do not have a significant effect on the objective function and thus can be left out of the surrogate (FORRESTER; SÓBESTER; KEANE, 2008).

The number of samples is dependent on the complexity of the function to be approximated and has a great impact over the surrogate accuracy. In general, more information of the function is provided when more sample points are considered, however, at a higher expense. On the other hand, for low-dimension functions, after a certain sample size is reached, an increase in the number of sample points does not contribute much to the surrogate accuracy (WANG; SHAN, 2006). Amouzgar and Strömberg (2017) define medium sample sizes of $3.5k$ and $2.5k$ for low dimension (four design variables or less) and high dimension (more than four design variables) functions respectively, and high samples sizes of $6k$ and $5k$ for low dimension and high dimension functions respectively, with the coefficient k given by:

$$k = \frac{(m+1)(m+2)}{2} \tag{22}$$

where m is the number of variables.

For successful construction of a surrogate of the response of interest based on a limited number of expensive simulations, careful planning of the experiments (referred as design of experiments) is crucial. There are many sampling approaches (e.g. random, full factorial, orthogonal arrays, Latin Hypercube, importance sampling, sequential or adaptive methods) (WANG; SHAN, 2006) and a robust sampling technique is desired to avoid dependency of the surrogate.

Evaluating the objective function for every possible combination of every possible design variable (which is referred as a full factorial design) (Figure 14) may be computational expensive. Although such design satisfies the uniformity criterion, it is only defined for designs of certain sizes (those that can be written as products of the numbers of levels for each dimension) and can lead to an unmanageably large number of samples (FORRESTER; SÓBESTER; KEANE, 2008). On the contrary, in a random sampling there is no uniformity, since the points are randomly defined within the variables bounds.

Among the sampling strategies, Latin Hypercube designs have become very popular. For an experimental design with p points in d dimensions, Latin Hypercube Sampling (LHS) is constructed in such a way that each of the d dimensions is divided into p equal levels or bins and that there is only one sample at each level (VIANA, 2013). In other words, since LHS is a stratified sampling approach, it is ensured that all portions of a given partition are

sampled (QUEIPO *et. al*, 2005). Figure 15 illustrates this feature for a ten-point LHS for a problem with three variables.

Figure 14. Example of a three-dimensional full factorial sampling

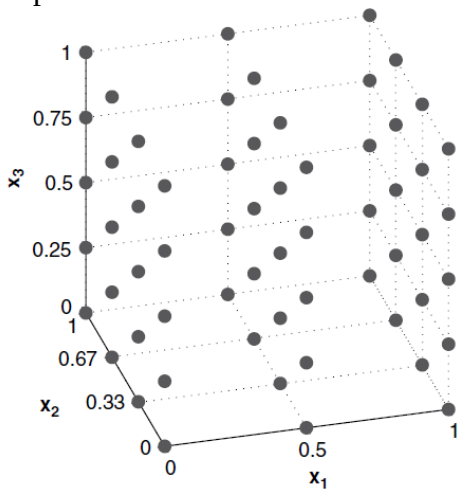

Source: Forrester, Sóbester and Keane (2008).

Figure 15. Example of a three-dimensional, ten-point Latin Hypercube sampling

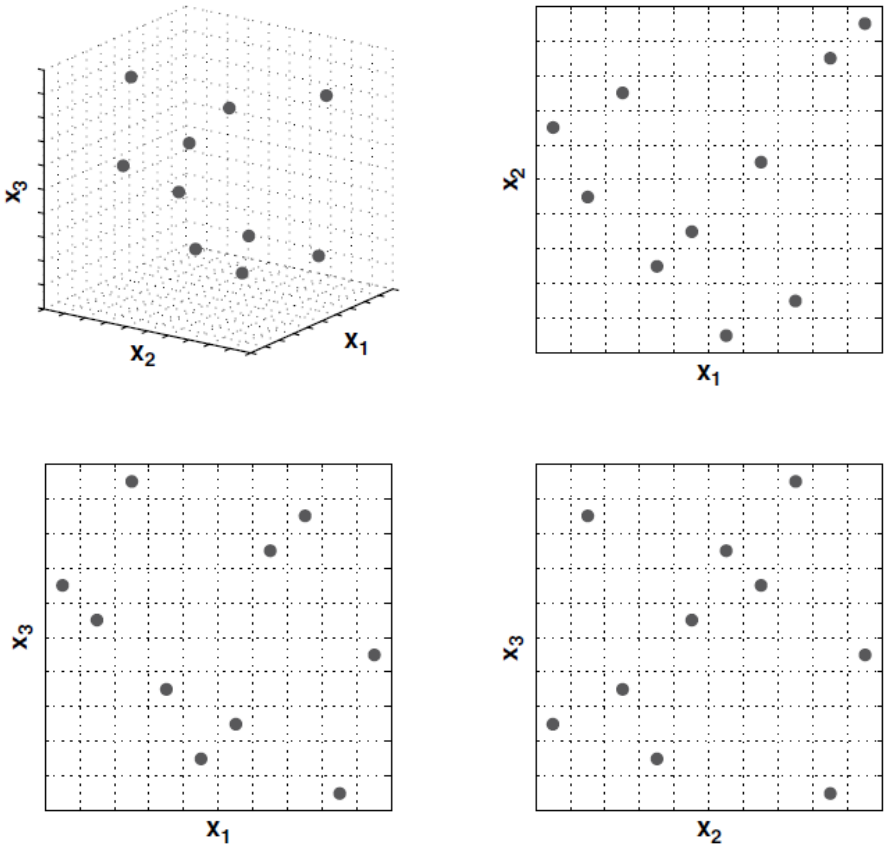

Source: Forrester, Sóbester and Keane (2008).

4.1.2 Choice of surrogate modelling approach

As mentioned, the surrogate modelling process starts with the identification of the variables that have a significant impact on the function to be approximated and the selection of a number of samples and sampling plan that represent the design domain as thoroughly as possible. The next step is the selection of a surrogate modelling technique, which is dependent on the problem size, the expected complexity and the cost of the analyses the surrogate is to be used in lieu of (FORRESTER; KEANE, 2009).

Other criteria that may be considered for proper selection of a surrogate modelling technique include: the functional form of the surrogate and its computational complexity, the robustness of the prediction away from the sampled data, the existence of software for computing the surrogate and characterizing its fit and prediction error (HUSSAIN; BARTON; JOSHI, 2002).

In the context of surrogate-based optimization (which refers to the idea of speeding optimization process by using surrogates for the objective functions and/or constraints), different modeling approaches have been shown to be effective (e.g. polynomial regression, RBF, Kriging, SVM) (QUEIPO *et. al*, 2005). Polynomial models, however, are unsuitable for the highly nonlinear and multidimensional engineering design problems (FORRESTER; SÓBESTER; KEANE, 2008). Alternatively, Kriging (one of the most complex surrogates) has the potential of providing more accurate predictions, but it can only be used for relatively low-dimensional problems due to the expense of training the model (FORRESTER; KEANE, 2009).

Among the available surrogate modelling techniques, RBFs have generated much interest because of its advantages over other techniques, such as the ability to effectively generate multi-dimensional interpolative approximation and versatility (MULLUR; MESSAC, 2005). In this work, RBF was utilized to construct a surrogate of the dynamic amplification factor. The purpose of the surrogate will be discussed in detail in Section 4.2, while this section will focus on the general description of the technique.

4.1.2.1 Radial Basis Functions

Given a set of samples x^i $(i = 1, \ldots, n_p)$ and the corresponding expensive function values $f(x^i)$, the objective is to obtain a global approximation function $\hat{f}(x)$, that accurately represents the original function over a given design domain. In an interpolating surrogate the function and the approximation are equal at all of the prescribed sample points:

$$\hat{f}(x^k) = f(x^k), \text{ for } k = 1,...,n_p \tag{23}$$

A radial basis function (RBF) $\hat{f}$ has the form

$$\hat{f}(x) = \sum_{i=1}^{n_p} \sigma_i \psi\left(\left\|x - x^i\right\|\right) \tag{24}$$

where σ_i are unknown coefficients (weights) to be determined, x^i denotes the ith of the n_p prescribed data points (or basis function centers) and ψ is the n_p–vector containing the values of the basis functions ψ themselves, evaluated at the Eucledian distances between the point x and the centres x^i of the basis functions.

There are many variations of RBFs in the literature, but the main difference is if the model is based on approximation or interpolation. In the case of interpolative RBF, it is assured that the surrogate solution at the training points is exact. On the other hand, in the case of approximation, the weights are obtained through least squares method, and the surrogate solution at the training points is not exact.

The basis functions ψ can be linear, cubic, Gaussian, multiquadratic or inverse multiquadratic. For a Gaussian function,

$$\psi(r) = e^{\frac{-r^2}{2c^2}} \tag{25}$$

where c is a prescribed parameter ($c > 0$).

To calculate the coefficients, the constraint of Eq. (23) is enforced, resulting in a linear system of equations

$$\sum_{i=1}^{n_p} \sigma_i \psi\left(\left\|x^k - x^i\right\|\right) = f(x^k), \qquad k = 1,...,n_p \tag{26}$$

which can be written in matrix form as

$$[A]\{\sigma\} = \{F\} \tag{27}$$

where

$A_{ik} = \psi\left(\left\|x^k - x^i\right\|\right),\ i = 1,...,n_p,\ \ k = 1,...,n_p;$

$\{\sigma\} = \begin{bmatrix} \sigma_1 & \sigma_2 & ... & \sigma_{n_p} \end{bmatrix}^T$ and $\{F\} = \begin{bmatrix} f(x^1) & f(x^2) & ... & f(x^{n_p}) \end{bmatrix}^T$

Since the linear system of equation is square (the number of equations is equal to the number of unknowns), there exist a unique set of coefficients σ_i that solves the linear system. With the determined coefficients σ_i, Eq. (24) can be used to estimate the function value at any point in the design domain.

Amouzgar and Strömberg (2017) present a variation of the classical RBF of the form

$$\hat{f}(x) = \sum_{i=1}^{n_p} \sigma_i \psi\left(\left\|x - x^i\right\|\right) + b(x) \tag{28}$$

where *b(x)* is the bias, presented as a group of polynomial functions.

Mullur and Messac (2005) argue that the unique solvability may represent a potential drawback, since the designer cannot impose any requirement regarding the shape of the final surrogate because such surrogate is fully prescribed by a unique formulation. Since the typical RBF approach does not provide the capability of generating a surrogate of choice, the authors proposed a surrogate modeling method called the extended radial basis function (E-RBF).

In this methodology, the following approximation function is defined

$$\hat{f}(x) = \sum_{i=1}^{n_p} \sigma_i \psi\left(\left\|x - x^i\right\|\right) + \sum_{i=1}^{n_p} \phi_i\left(x - x^i\right) \tag{29}$$

where Φ_i are nonradial basis functions. Satisfying the condition of Eq. (23) and writing in matrix notation:

$$[A]\{\sigma\} + [B]\left\{\left(\alpha^L\right)^T \left(\alpha^R\right)^T \beta^T\right\}^T = \{F\} \tag{30}$$

with

$$\alpha^L = \left\{ \alpha_{11}^L \;\; \alpha_{12}^L \;\; \ldots \;\; \alpha_{1m}^L \;\; \ldots \;\; \alpha_{(n_p)(m)}^L \right\}^T_{(mn_p)x1}$$

$$\alpha^R = \left\{ \alpha_{11}^R \;\; \alpha_{12}^R \;\; \ldots \;\; \alpha_{1m}^R \;\; \ldots \;\; \alpha_{(n_p)(m)}^R \right\}^T_{(mn_p)x1}$$

$$\beta = \left\{ \beta_{11} \;\; \beta_{12} \;\; \ldots \;\; \beta_{1m} \;\; \ldots \;\; \beta_{(n_p)(m)} \right\}^T_{(mn_p)x1}$$

where α^L, α^R and β are the coefficients of nonradial basis function (MULLUR; MESSAC, 2005).

4.1.3 Model Training and Validation

The stage of model training comprises the determination of the weights σ_i, which are calculated differently depending on the RBF formulation. Once the surrogate has been built, it is necessary to validate the model and assess its accuracy by evaluating the error. In this stage, additional sample points (validation data set) may be employed to compare the obtained predicted function values and the real values.

When it is too costly to employ a separate validation data set, the cross-validation method can be used (FORRESTER; KEANE, 2009). In cross-validation, the surrogate training data is randomly split into q roughly equal subsets, then each of these subsets is removed in turn and the model is fitted to the remaining $q - 1$ subsets. When all subsets have been removed, n predictions $\hat{f}_i$ of the n observed data points f_i will have been calculated, and these are used to calculate the cross-validation error:

$$\varepsilon_{cv} = \frac{1}{n}\sum_{i=1}^{n_t}\left(f_i - \hat{f}_i\right)^2 \tag{31}$$

Two standard performance metrics are the Root Mean Squared Error (RMSE) and the Maximum Absolute Error (MAE). Accurate surrogates will have low values for these two error measures.

The RMSE is calculated by

$$\text{RMSE} = \sqrt{\frac{\sum_{i=1}^{n_t}\left(f_i - \hat{f}_i\right)^2}{n_t}} \tag{32}$$

and the MAE is defined by:

$$\text{MAE} = \max\left|f_i - \hat{f}_i\right| \tag{33}$$

where n_t is the test data size, f_i is the exact function value at the ith test point and $\hat{f}_i$ is the corresponding predicted function value.

4.2 Surrogates in riser design

In a riser design for certain scenario, there is a large number of alternative riser configurations. Analyzing all these alternatives using FEM can be time-consuming and may incur high computational cost. Therefore, the development of approximations models that can replace the expensive numerical simulation procedures is encouraged. This section will review how these techniques have been used and applied for the design of such offshore systems by some authors and discuss the details of the surrogate developed in this work.

With the objective of improving confidence in SCR fatigue design, Quéau (2015) developed an efficient method for the approximation of the maximum stress range in the touchdown zone of the riser by employing an ANN approach. The authors firstly conducted a sensitivity analysis study, in order to determine the contribution of certain dimensionless groups on the fatigue life of the riser. In order to construct the ANN, 57,023 SCR configurations were simulated using OrcaFlex (ORCINA, 2012) and the input and output of some of those cases

were used to train and test the ANN. For the construction of a first approximation model, a back-propagation artificial neural network was trained. For a more refined approximation, the authors proposed various approximation for different areas of the design space, which resulted in an improved approximation comprising a total of nine ANN. With this methodology, the authors were able to develop an approximation that successfully approximates over 99% of the cases of the database with an accuracy of ±5%.

Yang and Zheng (2011) employed a reliability-based design optimization (RBDO) methodology, which combines reliability-based design and optimization design, and replaced the finite element code used for the simulations with a surrogate. The authors compared three surrogate modelling approaches (second-order response surface model, fourth-order response surface model and Kriging) for approximating the structural weight of the riser and the stress along the riser. When comparing the performance of the surrogates to the analysis results obtained with a finite element model, the authors concluded that the approximation of the riser weight had high accuracy, while the accuracy of the approximation for the stress was inferior.

The association of surrogates with optimization tools based on evolutionary algorithms represents a promising tool in the context of riser design. Yang, Li and Park (2011) presents an optimization scheme for deepwater risers' design considering fatigue life constraints. The problem defined by the authors consist of finding riser coating material and thickness of riser segments that minimize riser weight by employing an approximated model that replaces the numerical analysis procedures. Strength criteria, as specified by DNV-FOS-201, and fatigue criteria are considered as constraints. For the construction of the surrogate using Kriging, the authors firstly select a number of design points using LHS at which the computationally expensive code analysis is performed. Then, response surfaces are established for the functional relationships between the design variables and objective function. Finally, an assessment of the accuracy of the approximation model is made. The optimization algorithm chosen by the authors was the Island-based Genetic Algorithm (IGA). The authors demonstrated an example for a riser with six segments and the results showed that the Kriging models were successfully used in the optimization design for deepwater risers with different thickness and coating for the segments.

Chen *et al.* (2015) developed an optimization design of steep wave riser for extreme shallow water based on RBF surrogate model approach. In the optimization model defined by the authors, the design variables are the upper catenary length, the buoyancy segment length, the lower catenary length and the horizontal distance from hang-off point to TDP. Constraints of dynamic maximum tension at riser top, hang-off angle, minimum clearance of sag bend and

seabed, and riser total length were adopted. A surrogate model that approximates the relationship between the design variables and the response of maximum dynamic curvature at the riser top was used to substitute expensive evaluations of the objective function. For the construction of the surrogate using RBF networks, firstly, 152 sample points were obtained through LHS. For each of those samples points, a numerical simulation using OrcaFlex (ORCINA, 2012) considering only one critical load case was performed. A hybrid optimization combining two algorithms, which are multi-island genetic (MIGA) and non-linear programming by quadratic Lagrangian (NLPQL), was adopted. An optimal design was found for the example of a steep wave for an urgent design for an oil spill incident in extreme shallow water, demonstrating the high accuracy and efficiency of the methodology employed by the authors.

As mentioned in Chapter 2, in riser design, dynamic analyses are conducted to account for the combined effect of waves and currents over the riser. The number of loading cases that needs to be considered in dynamic analyses can be large, depending on the environment in which the riser is going to be deployed and its metaocean data, and, therefore, this stage of riser design can become time-consuming. Since many riser designs are evaluated during the optimization process, we anticipated that creating an automation routine to link the optimization model and the marine analysis software FLEXCOM would negatively affect the efficiency of the optimization process. Therefore, based on the reviewed works and the potential of the association of surrogates with optimization algorithms, a surrogate for the prediction of the dynamic amplification factor was developed in this work to be utilized in the optimization model in the lieu of dynamic analysis with FLEXCOM.

4.2.1 Surrogate model for the dynamic amplification factor

In order to explore the potential of the technique, a simplified surrogate for prediction of the amplification factor was developed. A sensitivity analysis was conducted to determine the surrogate variables. For this, departing from the riser defined in Section 2.2.5, different parameters were varied, keeping riser total length, horizontal projection and water level unchanged. The dynamic analysis were performed in FLEXCOM, and regular waves analyses were carried out for five wave cycles with wave loading ramped up over one wave period. Then, the results for effective tension from the static and dynamic analysis were plotted together and the amplification factor was calculated as

$$\beta = \frac{\text{Dynamic response}}{\text{Static response}} \tag{34}$$

It was concluded that the parameters with greater influence are the riser outer diameter, the internal fluid density and the wave data (returning period and amplitude). Figure 16 illustrates some of the results obtained in the sensitivity study, for risers with outer diameter ranging from 0.3 to 0.4 m, full of oil/water and empty, wave periods (Ts) from 10 to 20s, and wave amplitude (H) from 5 to 8 m. It was also observed that the wave direction did not influence the dynamic amplification factor.

With the defined surrogate variables and the variables bounds (Table 14), 30 samples were generated using LHS function in Matlab (MATHWORKS, 2010). Figure 17 shows 2D projections of the sampling plan. Then, each of the samples were analyzed in FLEXCOM and then amplification factor was calculated as previously described.

Table 14. Metamodel variables and bounds

Variable	Minimum	Maximum
Wave amplitude (H)	5 m	8 m
Wave period (T_s)	10 s	20 s
Internal fluid density (ρ_{int})	0	1025 kg/m^3
Riser outer diameter (D_o)	0,26 m	0,5 m

Source: author.

Next, the sample points and the real function values (the dynamic amplification factors calculated with FLEXCOM), were used to train the surrogate. The first approach tested was the formulation RBF bias posteriori described in the work by Amouzgar and Strömberg (2017). Fifteen training points (randomly selected from a set of available simulation results) were used to validate the model. Due to the low size of the sampling plan, the RBF was not able to capture the behavior of the function. RSME and MAE of 9.8% and 23.4% were obtained, respectively. Although the RBF was capable of predicting the dynamic amplification factor accurately for some of the points (with errors between the real function value and the predicted value of less than 1%), the discrepancy for points near of any of the variables bounds was high (around ±23%).

Figure 16. Results obtained with the sensitivity study (a) Do = 0.3m, riser full of oil; (b) Do = 0.3m, riser full of water; (c) Riser Do = 0.3m, empty riser; (d) Do = 0.4m, riser full of oil; (e) Do = 0.4m, riser full of water; (f) Do = 0.4m, empty riser.

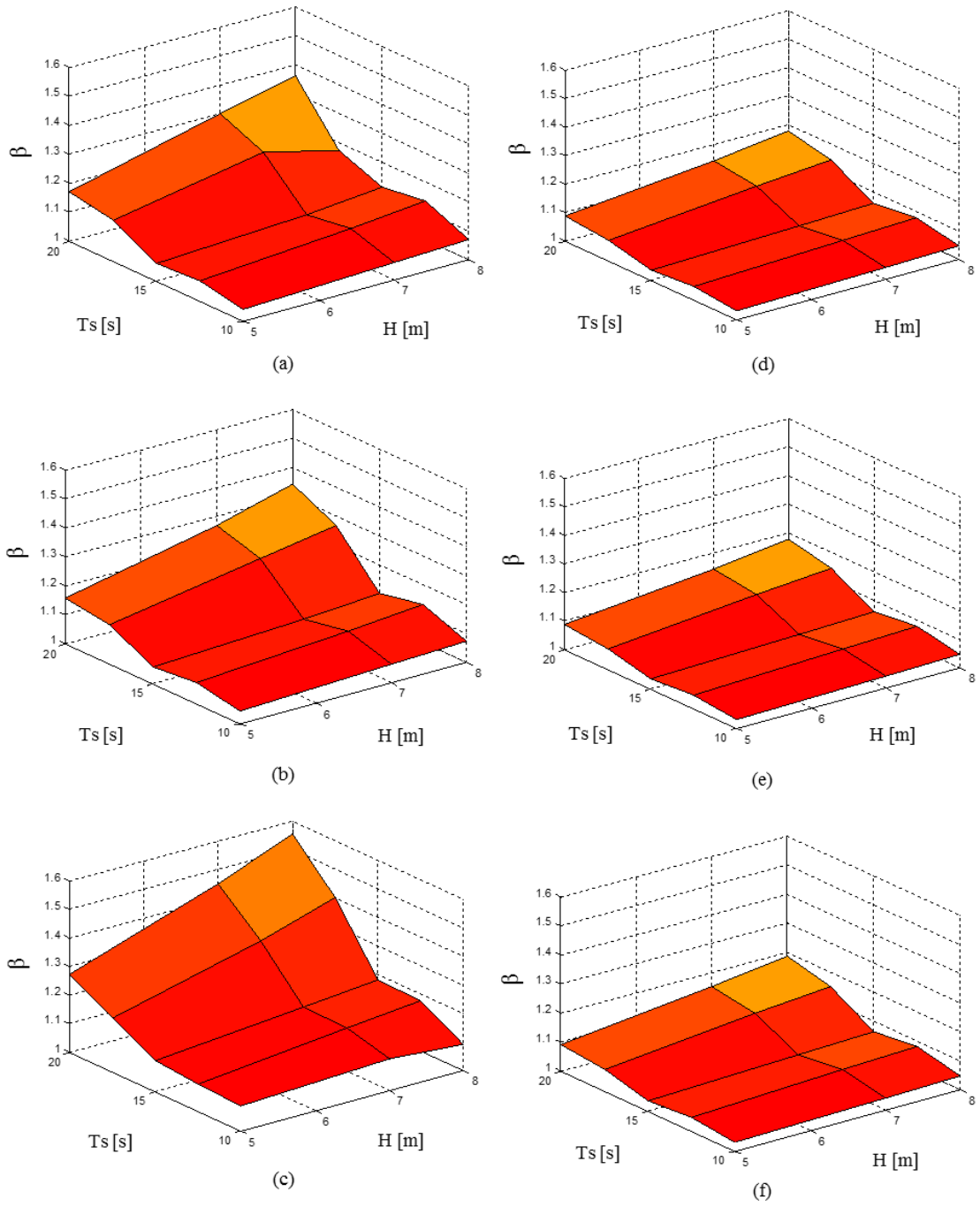

Source: author.

Figure 17. 2D projections of the LHS

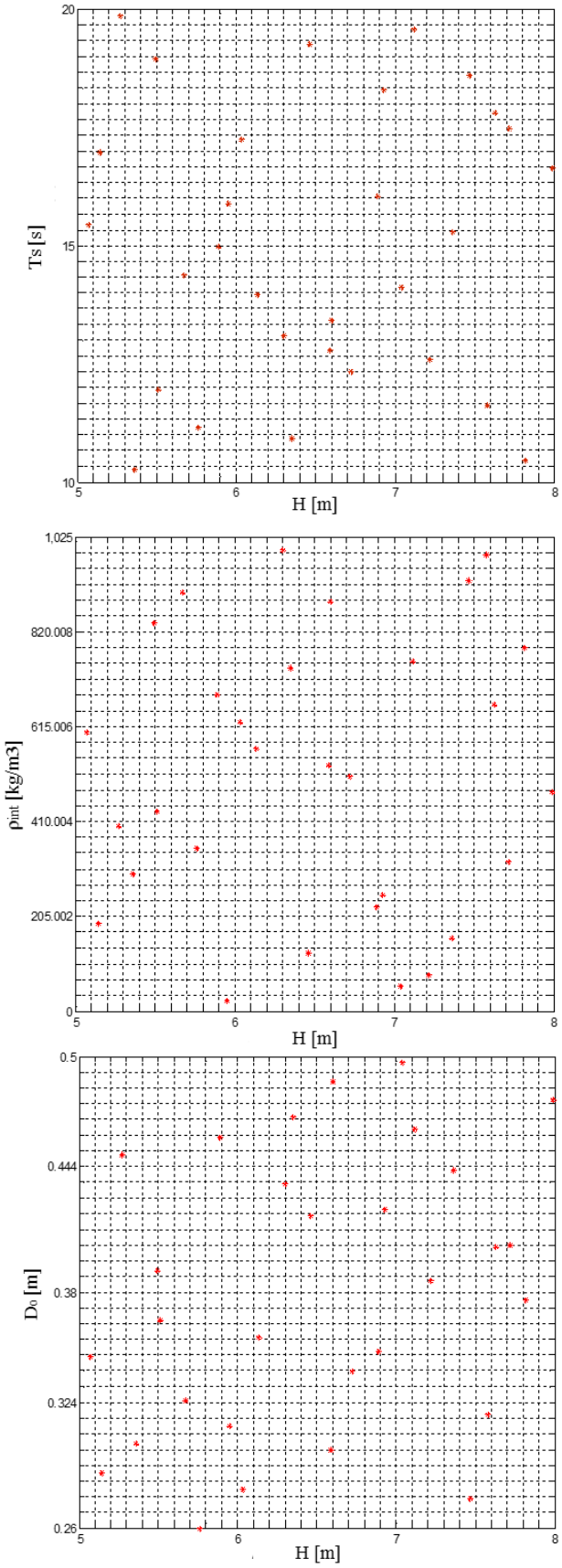

Source: author.

Given the unsatisfactory predictions obtained with the RBF bias posteriori formulation, the 30 samples points generated with LHS were used to train an E-RBF, as formulated in the work by Mullur and Messac (2005). This extended formulation, which encloses the simplified RBF formulation, results in a greater system of linear equations to be solved, and its implementation is more sophisticated. Yet this approach resulted in somewhat better predictions. Table 18 illustrates the comparison of the dynamic amplification factors predicted by the E-RBF and obtained with FLEXCOM for the riser detailed in Section 3.2.5. The dynamic loads simulated are shown on Table 15, with wave data given in Table 16 and current data given in Table 17. Although this formulation is more complex that the RBF bias posteriori and the model training is computationally more expensive, the execution time of the optimizations with the associated surrogate is in the same range.

Although the trained surrogate is not very accurate (errors between the real function value and the predicted value are within ±15%), which is due to the low sample size, its association with the developed optimization model represents a promising tool, as will be demonstrated by the numerical examples.

Table 15. Dynamic load cases considered in the comparison between dynamic amplification factors predicted by E-RBF and obtained with Flexcom for the riser defined in Section 3.2.5

Load case	Internal fluid	Design pressure	Offset		Current		Wave	
			Direction	% SWL	Return period	Direction	Return period	Direction
13	Oil	30 MPa	near	8	10	E	100	W
14	Oil	30 MPa	near	8	100	E	10	W
15	Oil	30 MPa	far	8	10	W	100	E
16	Oil	30 MPa	far	8	100	W	10	E
17	Empty	0	near	8	10	E	100	W
18	Empty	0	near	8	100	E	10	W
19	Empty	0	far	8	10	W	100	E
20	Empty	0	far	8	100	W	10	E
21	Water	37.5 MPa	near	3	10	E	100	W
22	Water	37.5 MPa	near	3	100	E	10	W
23	Water	37.5 MPa	far	3	10	W	100	E
24	Water	37.5 MPa	far	3	100	W	10	E

Source: author.

Table 16. Wave data for the load cases considered in the comparison between dynamic amplification factors predicted by E-RBF and obtained with Flexcom for the riser defined in Section 3.2.5

Return period	Direction	Wave amplitude [m]	Wave period [s]
100	W	6.7	11.0
10	W	5.8	10.0
100	E	6.5	11.5
10	E	5.0	10.5

Source: author.

Table 17. Current data for the load cases considered in the comparison between dynamic amplification factors predicted by E-RBF and obtained with Flexcom for the riser defined in Section 3.2.5

Depth [m]	Velocity [m/s]			
	CE 10	CE 100	CW 10	CW 100
0	1.28	1.70	1.26	1.79
100	1.14	1.52	1.01	1.44
350	1.05	1.40	0.98	1.39
500	0.69	0.92	0.68	0.96
1000	0.53	0.70	0.47	0.67
1500	0.41	0.54	0.46	0.65

Source: author.

Table 18. Comparison of the dynamic amplification factor predicted by the E-RBF and calculated with FLEXCOM for the riser defined in Section 3.2.5

Load case	$\beta_{FLEXCOM}$	$\beta_{surrogate}$	Difference
13	1.21	1.21	0.0%
14	1.05	1.15	9.5%
15	1.29	1.18	-8.5%
16	1.06	1.13	6.6%
17	1.27	1.22	-3.9%
18	1.07	1.17	9.3%
19	1.40	1.19	-15.0%
20	1.07	1.17	9.3%
21	1.20	1.23	2.5%
22	1.05	1.17	11.4%
23	1.27	1.20	-5.5%
24	1.05	1.14	8.6%

Source: author.

5 NUMERICAL EXAMPLES AND DISCUSSION

With the objective of validating the proposed optimization model, different numerical examples were tested. The obtained results are discussed and the robustness of the implemented model is demonstrated.

In the first scenario, with water level of 1500 m, three SCRs (with internal radius of 0.125 m) were optimized: the first case considers a SCR constituted of only one segment; the second case considers a SCR made up of three riser segments (with lengths of 800, 1000 and 720 m) of the same material; in the third case, the riser segments have the same length of case 2 but it is allowed the consideration of different materials for the segments. The surrogate model was not used for these examples.

The model parameters are shown on Table 19. The load effect factors for functional and environmental loads and the dynamic amplification factor are 1.1, 1.3 and 1.5, respectively. The surrogate model was not used in these examples and the value utilized for dynamic amplification factor was adopted from previous studies of Silva *et al.* (2013). Only 6 static load cases (Table 20) were considered and the current effect was ignored in these examples. The PSO and AG parameters are shown on Table 21. On the optimizations, the materials from Table 8 and thickness values of Table 9 were considered. The material properties given on Table 10 and relative costs given on Table 22 were used in the input file of the optimization.

Table 19. Model parameters - SCR for Scenario 1

Parameter	Symbol	Value
Gravity acceleration	g	9.81 m/s²
Water density	ρ_{water}	1025 kg/m³
Still water level	SWL	1500 m
Connection coordinates	(x_{con}, y_{con})	(0m, 1500m)
Horizontal projection	HP	1732m
Safety class factor	γ_{SC}	1.14
Material resistance factor	γ_m	1.15
Buckling propagation factor	γ_c	1.0
Material strength factor	α_U	0.96
Material fabrication factor	α_{fab}	0.85
Temperature derating factor for the yield stress	$f_{y,temp}$	0.0
Temperature derating factor for the tensile strength	$f_{u,temp}$	0.0

Source: author.

Table 20. Load cases - SCR for Scenario 1

Load case	Offset	Direction	Internal fluid density	Pressure at riser top	Current
1	8.5%	near	880 kg/m³	30 MPa	0 m/s
2	8.5%	far	880 kg/m³	30 MPa	0 m/s
3	8.5%	near	0	0	0 m/s
4	8.5%	far	0	0	0 m/s
5	3.0%	near	1025 kg/m³	37.5 MPa	0 m/s
6	3.0%	far	1025 kg/m³	37.5 MPa	0 m/s

Source: author.

Table 21. Parameters of the optimization algorithms

	GA	PSO
Crossover rate	0.90	0.90
Mutation rate	0.05	0.05
Swarm topology	NA	Gbest
Particle inertia	NA	Linear, varying from 0.9 to 0.4
Cognitive factor	NA	Linear, varying from 2.5 to 0.0
Social factor	NA	Linear, varying from 0.0 to 2.5

Source: author.

Table 22. Relative cost of the materials – Case 1

Classification	Relative cost (volumetric)
B	1,00
X42	1,20
X46	1,32
X52	1,49
X56	1,60
X60	1,72
X65	1,86
X70	2,00
X80	2,29

Source: author.

For the first case, with the riser constituted of only one segment with total length of 2520 m, the optimum design, obtained with a population of 50 individuals and 25 generations, is a SCR made of API 5L X56 steel and wall thickness of 0.025 m, for which the objective function is 87.085. Both algorithms found this optimum solution, but convergence was achieved earlier for PSO.

For the second case, the optimum design is a SCR made of API 5L X46 steel and wall thickness of 0.030 m for the first segment and 0.0275 m for the second and third segments, for which the objective function is 82.298. Lastly, the optimum design for the third case is a riser in which the first segment is made of API 5L grade B steel and wall thickness of 0.035 m, the second segment is made of API 5L X46 steel and wall thickness of 0.0275 m and the third segment is made of API 5L grade B steel and wall thickness of 0.0325 m. Both algorithms found this optimum solution, but again convergence was achieved earlier for PSO.

The results for this scenario show that the adopted methodology of dividing the riser in segments represented an advantage, since it implied in overall reduction of riser cost. When comparing the solutions for the riser with one segment and the riser with three segments, a reduction of about 11% in the total cost of the riser was achieved. In terms of optimization, it can be seen that a better solution is found when multiple segments are admitted, since a larger search space is considered.

Then, optimization of SCRs for a scenario with water level of 2000 m, riser horizontal projection of 1909.3 m and total length of 3100 m was performed. The load cases of Table 20 were considered, but a polygonal current profile varying from 1.0 m/s at the sea top and 0 m/s at the sea bottom was applied. Again, the surrogate model was not used, but this time the amplification factor was 1.05 (based on the comparison study of the results obtained with inextensible cable model and FLEXCOM, which showed differences of less than 5%). A comparison was made for different pricing cases of materials.

Considering the costs given on Table 22, for a riser with only one segment, the optimum design is a riser made of API 5L grade B steel and wall thickness of 0.0375 m (with objective function 104.998). Taking into account a reduction in material costs, as shown on Table 23, the optimum design is a riser made of API 5L X46 steel and wall thickness of 0.0325 m (with objective function 102.828). Although the cost difference between the optimum designs obtained with the two pricing cases was small, this comparison shows that a reduction in the price of the steels favored the utilization of a superior steel grade, with higher resistance, implying in reduction of riser wall thickness.

For the same scenario, a SCR with three segments (930, 1270 and 900 m), was optimized. The optimum design for this case is a riser in which the first segment is made of API 5L X60 steel and wall thickness of 0.022 m, the second segment is made of API 5L X52 steel and wall thickness of 0.030 m and the third segment is made of API 5L grade B steel and wall thickness of 0.045 m (objective function 102.472). Although this example allowed the adoption of materials with higher resistances to be used just in the portions of the riser with higher

requirements, the possibility of dividing the riser in segments was less advantageous than in the first scenario, when referring to cost reduction.

Table 23. Relative cost of the materials – Case 2

Classification	Relative cost (volumetric)
B	1,00
X42	1,10
X46	1,15
X52	1,20
X56	1,28
X60	1,38
X65	1,49
X70	1,80
X80	2,00

Source: author.

Later, the optimization of SCRs for a scenario with water level of 2000 m, riser horizontal projection of 1909.3 m and total length of 3400 m, with more load cases was performed. First, the static and quasi-static load cases of Table 11 (with current data given on Table 24) were considered. Initially, the surrogate model was not used and the dynamic amplification factor was considered as 1.5 for all load cases. The relative costs given on Table 23 were adopted. The optimum design for this case is a riser made of API 5L X65 steel and wall thickness of 0.030 m (objective function 133.689). For optimizations with 50 generations and 25 individuals, both algorithms found this optimum design, but for PSO the convergence was achieved in the 5nd generation, while, for GA, the convergence was achieved in the 7th generation.

Then, the dynamic load cases given on Table 15 were input in the optimization file, along with the previous static and quasi-static load cases (Table 11). The dynamic amplification factor was considered 1.05 for the static and quasi-static load cases (to account for the difference between the results obtained with the inextensible cable model and FLEXCOM) and the E-RBF (trained outside of the optimization procedure) was utilized for the prediction of the dynamic amplification factor in the dynamic load cases. The optimum design for this case is a riser made of API 5L X56 steel and wall thickness of 0.030 m (objective function 114.847).

The comparison of the last two examples shows that the introduction of the E-RBF for the prediction of the dynamic amplification factor was important to refinement of the model,

since the previous methodology of considering the dynamic amplification factor as 1.5 can lead to overly conservative riser designs. In these examples, the consideration of the surrogate model lead to a reduction of 16.4% in the objective function.

Lastly, to validate the latter optimized riser design, a model for it was build in FLEXCOM, all the load cases were simulated and code checking was performed. Maximum LFRD for the cases were in accordance with the technical standard, with maximum values occurring in the TDZ. Figures 18, 19 and 20 illustrates the maximum LFRD obtained with FLEXCOM for some of the load cases.

Ultimately, the efficiency of the optimization process is demonstrated by a comparison of execution time. Simulating each static and dynamic load case take 2 seconds and 50 seconds, respectively, in FLEXCOM. Thus, analyzing all the 24 load cases previously defined for a riser design in FLEXCOM would take approximately 10.4 minutes. In an optimization with 50 generations and 25 individuals, 1275 possible riser designs are evaluated, and if the analysis was performed using FLEXCOM, it would take 221 hours to finish it. Nonetheless, the optimization process with the consideration of the inextensible cable model and the surrogate model, is concluded within 5 to 12 minutes, depending if the riser is has one or multiple segments.

Table 24. Current data – Scenario with water depth of 2000 m

Depth [m]	Velocity [m/s]					
	CE 1	CE 10	CE 100	CW 1	CW10	CW 100
0	0.96	1.35	1.77	1.05	1.32	1.83
500	0.85	1.28	1.70	0.97	1.26	1.79
600	0.76	1.14	1.52	0.78	1.01	1.44
850	0.70	1.05	1.40	0.75	0.98	1.39
1000	0.46	0.69	0.92	0.52	0.68	0.96
1500	0.35	0.53	0.70	0.36	0.47	0.67
2000	0.27	0.41	0.54	0.35	0.46	0.65

Source: author.

Table 25. Wave data – Scenario with water depth of 2000 m

Return period	Direction	Wave amplitude [m]	Wave period [s]
100	W	6.7	11.5
10	W	5.8	10.5
100	E	6.5	12.0
10	E	5.4	10.5

Source: author.

Figure 18. DNV code checking using FLEXCOM – Load cases n° 7, 8, 11, 12

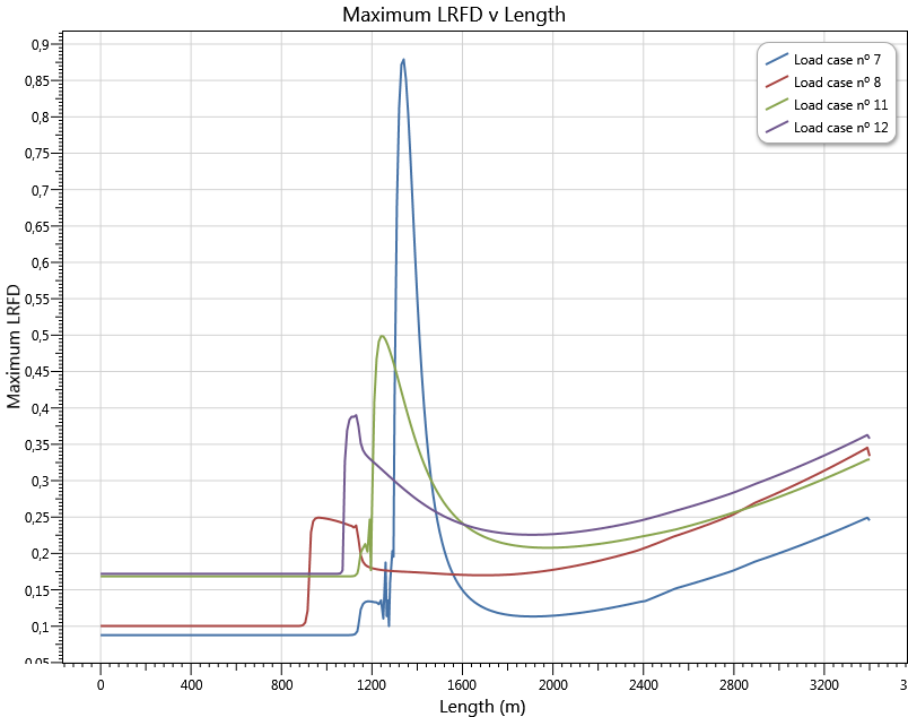

Source: imported from FLEXCOM.

Figure 19. DNV code checking using FLEXCOM – Load cases n° 13 to 16

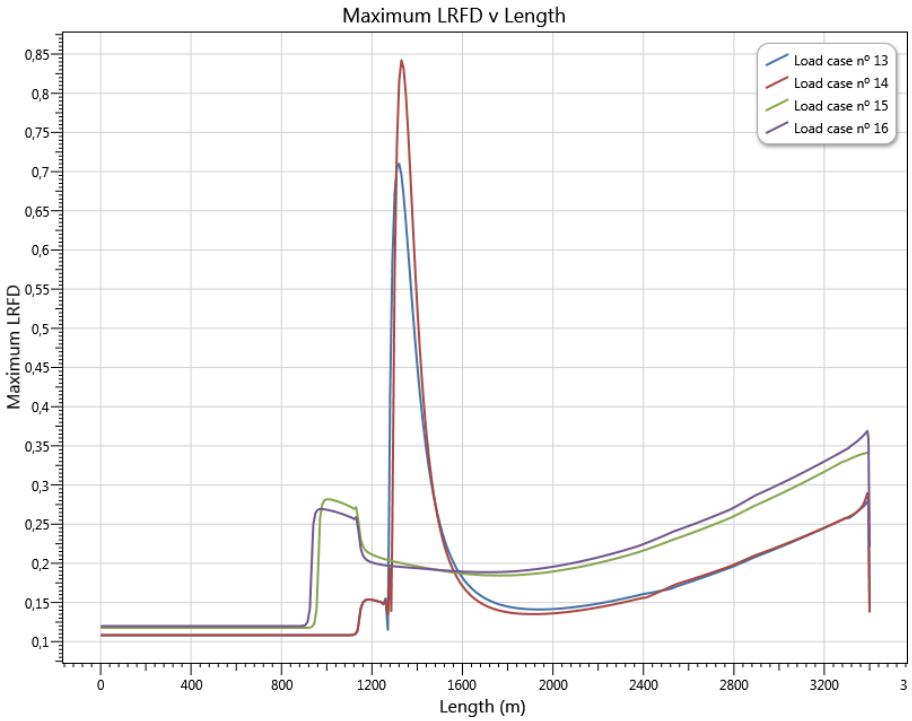

Source: imported from FLEXCOM.

Figure 20. DNV code checking using FLEXCOM – Load cases n° 21 to 24

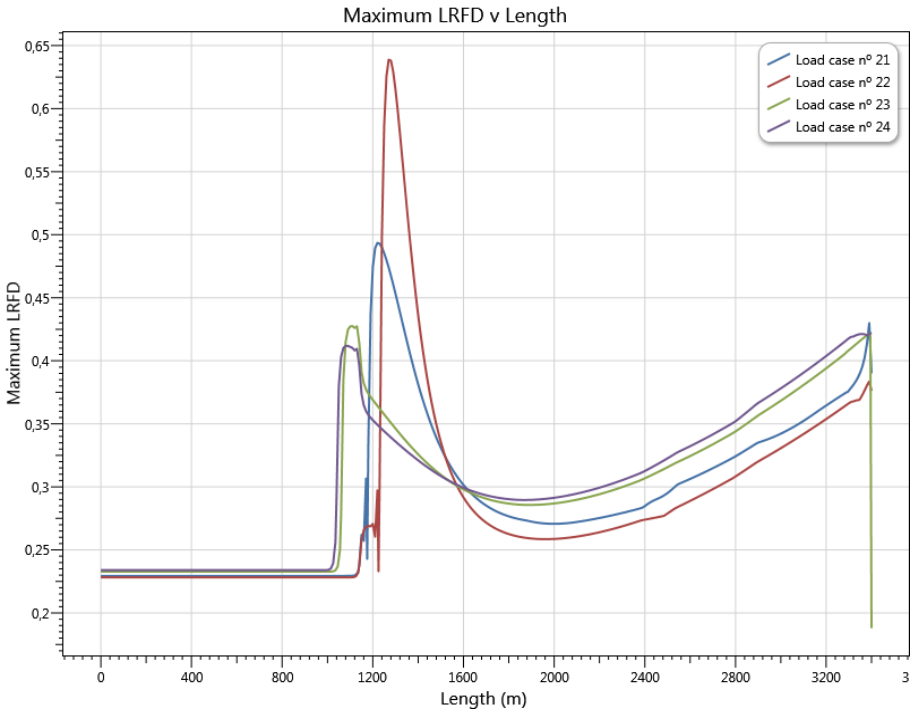

6 CONCLUSIONS

In this work, a preliminary model for design of steel catenary risers using bio-inspired optimization algorithms was developed and implemented. In the optimization model, the choice of using an inextensible cable model for analysis of static and quasi-static load cases proved to be adequate, with differences of ± 5% in comparison to FE analysis. A surrogate model for the dynamic amplification factor, utilized in lieu of dynamic analyses, was introduced for refinement of the model. Although the sampling size used for surrogate training was small and the prediction near the variables bounds are not very accurate, the potential of the association of surrogate models and optimization tools was demonstrated.

Optimum solutions, which represent the riser with the lowest value for the objective function that fulfills requirements of the technical standards for the specified conditions, were found for all the numerical examples presented by both algorithms tested, proving the robustness of the proposed methodology and its computer implementation. The numerical examples herein presented also demonstrated the flexibility of the optimization model in terms of problem definition. In addition, this preliminary model is not dependent on designer's experience and it allows this activity to be conducted within an acceptable execution time: it can obtain viable riser designs in a period 18 times lower than if the traditional methodology of trial and error is employed.

Suggestions for future work include:

- Refinement of the surrogate model for the dynamic amplification factor: addressing other sampling techniques, the effect of sampling size over the surrogate accuracy, comparison of different surrogate modelling techniques.
- Incorporation of a model for optimization of steel lazy-wave risers, to provide the designer with SLWR and SCR designs for given input data.
- Include in the optimization model the concept of weight-optimized risers using clump weights, to analyze how it can improve SCR response in deepwater applications.
- Elaboration of a surrogate model for maximum dynamic stress amplitude, to be utilized in lieu of fatigue analysis.

REFERENCES

ADEYEMI, B. J.; SULAIMON, A. A. Predicting wax formation using artificial neural network. *In*: Nigeria Annual International Conference and Exhibition, 2012, Lagos.

ADHAV, R.; SAMAD, A.; KENYERY, F. 2015. Design optimization of electric centrifugal pump by multiple surrogate models. *In*: SPE Middle East Oil & Gas Show and Conference, 2015, Manama.

ALBRECHT, C. H. **Evolutionary algorithms applied to mooring synthesis and optimization** (in Portuguese). 2005. Doctoral thesis – Universide Federal do Rio de Janeiro, Rio de Janeiro, 2005.

ALVES, J. C.; PARENTE JR., E. Analise numérica de risers utilizando um modelo de cabo inextensível. *In*: XXXVII Iberian Latin American Congress on Computational Methods in Engineering, 2016, Brasília.

AMERICAN BUREAU OF SHIPPING. **Guide for Building and Classing Subsea Riser Systems**. 2014.

AMERICAN PETROLEUM INSTITUTE. **Recommended Practice 2RD - Design of Risers for Floating Production Systems (FPSs) and Tension-Leg Platforms (TLPs)**. 1998.

AMERICAN PETROLEUM INSTITUTE. **Specification 5L - Specification for Line Pipe**. 2004.

AMOUZGAR, K.; STROMBERG, N. Radial basis functions with a priori bias in comparison with a posteriori bias under multiple modeling criteria. **Structural and Multidisciplinary Optimization**, v. 55, issue 4, p. 1453-1469, 2016.

ARORA, J. S. **Introduction to Optimum Design**. 3rd ed. 2012.

BAI, Y., BAI, Q. **Subsea Pipelines and Risers**. 1st ed. 2005.

BAI, Y., BAI, Q. **Subsea Structural Engineering**. 1st ed. 2010.

BARROSO, E. S. **Análise e otimização de estruturas laminadas utilizando a formulação isogeométrica**. 2015. Dissertation (Master in Civil Engineering) – Universidade Federal do Ceará, Fortaleza, 2015.

BARROSO, E. S.; PARENTE JR., E.; MELO, A. M. C. A hybrid PSO-GA algorithm for optimization of laminated composites. **Structural and Multidisciplinary Optimization**, v. 55, issue 6, p. 2111-2130, 2017.

BRATTON, D.; KENNEDY, J. Defining a standard for particle swarm optimization. *In*: IEEE Swarm Intelligence Symposium, 2007, Honolulu.

CHAKRABARTI, S. K. **Handbook of Offshore Engineering**. 1st ed. 2005.

CHANDRASEKARAN, S.; JAIN, A. K. **Ocean Structures: Construction, Materials, and**

Operations. 2016.

CHATTERJEE, A.; SIARRY, P. Nonlinear inertia weight variation for dynamic adaptation in particle swarm optimization. **Computers & Operations Research**, v. 33, p. 859-871, 2006.

CHEN, J.; YAN, J.; TANG, M.; YANG, Z.; YUE, Q. Riser configuration design for extreme shallow water with surrogate model based optimization. *In*: ASME 2015 34th International Conference on Ocean, Offshore and Arctic Engineering, 2015, St. John's.

DE ANDRADE, E. Q.; DE AGUIAR, L. L.; SENRA, S. F.; SIQUEIRA, E. F. N.; TORRES, A. L. F. L.; MOURELLE, M. M. Optimization procedure of steel lazy wave riser configuration for spread moored FPSOs in deepwater offshore Brazil. *In*: Offshore Technology Conference, 2010, Houston.

DET NORSKE VERITAS. **Offshore standard F101**: Submarine Pipeline Systems. 2013.

DET NORSKE VERITAS. **Offshore standard F201**: Dynamic Risers. 2010a.

DET NORSKE VERITAS. **Recommended practice C203**: Fatigue Design of Offshore Steel Structures. 2011.

DET NORSKE VERITAS. **Recommended practice F204**: Riser Fatigue. 2010b.

EBERHARDT, R. C.; SHI, Y. Comparing inertia weights and constriction factors in particle swarm optimization. *In*: IEEE international conference on evolutionary computation, 2000, San Diego.

EL-SEBAKHY, E. A.; SHELTAMI, T.; AL-BOKHITAN, S. Y.; SHAABAN, Y.; RAHARJA, P. D.; KHAERUZZAMAN, Y. Support Vector Machines framework for predicting the PVT properties of crude oil systems. *In*: SPE Middle East Oil and Gas Show and Conference, 2007, Manama.

ESTECO. 2009. modeFRONTIER 4.1 User Manual.

FORRESTER, A. I. J.; KEANE, A. J. Recent advances in surrogate-based optimization. **Progress in Aerospace Sciences**, v. 45, p. 50-79, 2009.

FORRESTER, A. I. J.; SÓBESTER, A.; KEANE, A. J. **Engineering Design via Surrogate Modelling**. 2008.

FROUFE, L. M. **Análise comparativa de critérios de dimensionamento de risers rígidos**. 2006. Dissertation (Master in Oceanic Engineering) - Universidade Federal do Rio de Janeiro, Rio de Janeiro, 2006.

HE, S.; Wu, Q. H.; WEN, J. Y.; SAUNDERS, J. R.; PATON, R. C. A particle swarm optimizer with passive congregation. **BioSystems**, v. 78, p. 135-147, 2004.

HOROWITZ, B.; AFONSO, S. M. B.; MENDOÇA, C. V. P. Surrogate based optimal waterflooding management. **Journal of Petroleum Science and Engineering**, v. 112, p. 206-219, 2013.

HUSSAIN, M. F.; BARTON, R. R.; JOSHI, S. B. Metamodeling: radial basis functions, versus polynomial. **European Journal of Operational Research**, v. 138, p. 142-154, 2002.

KARUNAKARAN, D.; MELING, T. S.; KRISTOFFERSEN, S.; LUND, K. M. Weight-optimized SCRs for deepwater harsh environments. *In*: Offshore Technology Conference, 2005, Houston.

KONGSBERG. Dynamic positioning - basic principles. Available at: <https://www.km.kongsberg.com/ks/web/nokbg0240.nsf/AllWeb/BD306BBB3E7DA73FC1256DAB00353083?OpenDocument>. Accessed on March 25, 2016.

LARSEN, C. M.; HANSON T. Optimization of catenary risers. **Journal of Offshore Mechanics and Arctic Engineering**, v. 121, p. 90-94, 1999.

LEFFLER, W. L.; PATTAROZZI, R.; STERLING, G. **Deepwater Petroleum Exploration & Production**: A Nontechnical Guide. 2003.

LIND, Y. B.; KABIROVA, A. R. Artificial neural networks in drilling troubles prediction. *In*: SPE Russian Oil and Gas Exploration & Production Technical Conference and Exhibition, 2014, Moscow.

LONG, W.; CHAI, D.; AMINZADEH, F. Pseudo density log generation using artificial neural network. *In*: SPE Western Regional Meeting, 2016, Anchorage.

MATHWORKS INC. 2010. MATLAB optimization toolbox user's guide.

McDONALD, D. B.; GRANTHAM, W. J.; TABOR, W. L.; MURPHY, M. J. Global and local optimization using radial basis function response surface models. **Applied Mathematical Modelling**, v. 31, p. 2096-2110, 2007.

MCS KENNY. 2013. Flexcom User Manual. Version 8.

MULLUR, A. A.; MESSAC. A. Extended radial basis functions: more flexible and effective metamodeling. **AIAA Journal**, v. 43, No. 6, p. 1306-1315, 2005.

OKPO, E. E.; DOSUNMU, A.; ODAGME, B. S. Artificial neural network model for predicting wellbore instability. *In*: SPE Nigeria Annual International Conference and Exhibition, 2016, Lagos.

ORCINA. OrcaFlex User Manual 9.5. UK, 2012.

PETROBRAS. 2001. ANFLEX: A program for Risers and Mooring Lines Analysis, User's and Theoretical Manual.

PINA, A. A.; ALBRECHT, C. H.; LIMA, B. S. L. P.; JACOB, B. P. Tailoring the particle swarm optimization algorithm for the design of offshore oil production risers. **Optimization and Engineering**, v. 12, n. 1-2, p. 215-235, 2011.

PINA, A.A.; MONTEIRO, B. F.; ALBRECHT, C. H.; LIMA, B. S. L. P.; JACOB, B. P., 2016.

Artificial neural networks for the analysis of spread-mooring configurations for floating production systems. **Applied Ocean Research**, v. 59, p. 254-264, 2016.

PINTO, J. W. O. **Uso de otimização sequencial aproximada a problemas uni e multiobjetivos de gerenciamento de reservatórios**. 2014. Dissertation (Master in Civil Engineering) -Universidade Federal do Pernambuco, Recife, 2014.

QUEÁU, L. M. **Estimating the fatigue damage of steel catenary risers in the touchdown zone.** 2015. Doctoral thesis - The University of Western Australia, Perth, 2015.

QUEIPO, N. V.; HAFTKA, R. T.; SHYY, W.; GOEL, T.; VAIDYANATHAN, R.; TUCKER, P. K. Surrogate-based analysis and optimization. **Progress in Aerospace Sciences**, v. 41, p. 1-28, 2005.

RANJAN, A.; VERMA, S.; SINGH, Y. Gas lift optimization using Artificial Neural Network. *In*: SPE Middle East Oil & Gas Show and Conference, 2015, Manama.

RATNAWEERA, A.; HALGAMUGE, S. K.; WATSON, H. C. Self-organizing hierarchical particle swarm optimizer with time-varying acceleration coefficients. Transactions on Evolutionary Computation, v. 8, p. 240–255, 2004.

ROCHA, I. B. C. M. **Análise e otimização de cascas laminadas considerando não-linearidade geométrica e falha progressiva**. 2013. Dissertation (Master in Civil Engineering) – Universidade Federal do Ceará, Fortaleza, 2013.

RUSWANDI, M. I. **Improvisation of deepwater weight distributed steel catenary riser**. 2009. Dissertation (Master in Offshore Technology) – The University of Stavanger, Stavanger, 2009.

SAGLAR, N.; TOLEMAN, B.; THETHI, R. Frontier deepwater developments - the impact on riser systems design in water depths greater than 3000m. *In*: Offshore Technology Conference, 2015, Houston.

SILVA, R. F.; TEÓFILO, F. A. F.; PARENTE JR., E.; MELO, A. M. C.; HOLANDA, A. S. Optimization of composite catenary risers. **Marine Structures**, v. 33, p. 1-20, 2013.

SIMPSON, T. W.; PEPLINSKI, J. D.; KOCH, P. N.; ALLEN, J. K. Metamodels for computer-based engineering design: survey and recommendations. **Engineering with Computer**, vol 17, p. 129-150, 2001.

TANAKA, R. L. **Otimização da configuração de risers rígidos**. Doctoral thesis - Escola Politécnica da Universidade de São Paulo, São Paulo, 2009.

TANAKA, R. L.; MARTINS, C. A. Dynamic optimization of steel risers. *In*: Seventh International Offshore and Polar Engineering Conference, 2007, Lisbon.

TENARIS. High strength tubular steels for riser systems. Available at: <www.tenaris.com/en/Products/OffshoreLinePipe/Risers.aspx>. Accessed on March 25, 2016.

VANDIVER, J. K. User Guide for SHEAR7, Version 4.5. Massachusetts Institute Technology, 2007.

VIANA, F. A. C. 2013. Things you wanted to know about the Latin hypercube design and were afraid to ask. *In*: 10th World Congress on Structural and Multidisciplinary Optimization, 2013, Orlando.

VIEIRA, I. N. **Algoritmos bio-inspirados aplicados a otimização de risers rígidos em catenária**. 2009. Dissertation - Universidade Federal do Rio de Janeiro, Rio de Janeiro, 2009.

VIEIRA, I. N., LIMA, B. S. L. P. & JACOB, B. P. Bio-inspired algorithms for the optimization of offshore oil production systems. **International Journal for Numerical Methods in Engineering**, v. 91, p. 1023-1044, 2012.

VINNEM, J.E. **Offshore Risk Assessment**: principles, modelling and application of QRA studies. 2007.

WANG, G. G.; SHAN, S. Review of metamodeling techniques in support of engineering design optimization. **Journal of Mechanical Design**, v. 129, p. 370-380, 2006.

WANG, P. **Development and applications of production optimization techniques for petroleum fields**. 2003. Doctoral thesis - Stanford University, Stanford, 2003.

WANG, X.; FENG, Q.; HAYNES, R. D. Optimization of well placement and production for large-scale mature oil fields. **Journal of Engineering Science and Technology Review**, v. 8, p. 134-140, 2015.

YANG, H.; LI, H.; PARK, H. Optimization design for steel catenary riser with fatigue constraints. **International Journal of Offshore and Polar Engineering**, v. 21, p. 302-307, 2011.

YANG, H.; ZHENG, W. Metamodel approach for realiability-based design optimization of a steel catenary riser. **Journal of Marine Science and Technology**, v. 16, p. 202-213, 2011.

ZHAO, T.; JAYARAM, V.; MARFURT, K. J.; ZHOU, H. Lithofacies classification in Barnett shale using proximal Support Vector Machines. *In*: Society of Exploration Geophysicists Annual Meeting, 2014, Denver.

APPENDIX A – STRUCTURE OF THE INPUT FILES OF THE OPTIMIZATION PROCEDURE

The general structure of the input files (.ris and .opt) is composed of %KEYWORDS followed by the associated data. Integer and real values are herein indicated as [data] and <data>, respectively. Strings should be written in the input file between ' ' and are indicated in the as 'data'. The end of the input file is indicated by the keyword %END. All data after the %END keyword is not the read by the program. The keywords and associated data of each input file will be presented in the following.

The algorithm variables are defined in the .opt file. The keywords and input data of the file are described in the following table.

Table 26. Structure of the .opt file

%HEADER This section must be in the beginning of the file and must contain any relevant information about the current file. %PROBLEM.TYPE 'SCR' %OPTIMIZATION.ALGORITHM 'StdGA' 'StdPSO' %INDIVIDUAL.TYPE 'IntegerMatrix' %OPTIMIZATION.NUMBER [optimization number] %MAXIMUM.GENERATIONS [maximum generations] %POPULATION.SIZE [population size] %MIGRATION.GENERATION.GAP [migration generation gap] %MIGRATION.INDIVIDUAL.NUMBER [migration individual number] %CONSTRAINT.TOLERANCE <constraint tolerance>

%SELECTION.METHOD
'Ranking'
'FitnessProportional'

%CROSSOVER.RATE
<crossover rate>

%MUTATION.PROBABILITY
<mutation probability>

%SWARM.TOPOLOGY
'Square'
'Ring'
'Gbest'

%PARTICLE.INERTIA
'CONSTANT' 0.72

%COGNITIVE.FACTOR
'CONSTANT' 1.5

%SOCIAL.FACTOR
'CONSTANT' 1.5

%END

The data that should be included in the .ris file for the optimization of SCRs is described in the following table. These include the keywords for the definition of the riser parameters and the keywords for reading the surrogate trained out of the optimization procedure.

Table 27. Structure of the .ris file

%HEADER This section should be in the beginning of the file and should contain any relevant information about the current file. %MATERIAL [number of materials] %MATERIAL.ISOTROPIC [number of materials] [material label] <Young's modulus> <Poisson's ratio> <yield stress> <tensile strength> %MATERIAL.DENSITY [number of materials] [material label] <material density> %MATERIAL.COST

[number of materials]
[material label] <material cost>

%RISER.PARAMETERS
<gravity acceleration>
<water density>
<still water level>

%RISER.CABLE.PARAMETERS
[cable definition] (1 = defined by top angle; 2 = defined by horizontal projection)
[anchor position] (1 = suspended anchor; 2 = anchor fixed to seabed)
<x coordinate of connection> <y coordinate of connection>
<top angle or horizontal displacement>

%RISER.LOAD.CASES
[number of load cases]
[load case index] [load type (1 = static; 2 = dynamic)] <offset> <internal fluid density> <internal pressure at the top> <amplification factor> <functional loads factor> <environmental loads factor> [current profile index] [wave profile index]

%RISER.CURRENT.PROFILES
[number of current profiles]
[current profile sequential index] [number of points]
<y coordinate of the first point> <velocity at first point>
<y coordinate of the nth point> <velocity at nth point>

%RISER.WAVE.PROFILES
[number of wave profiles]
[wave profile index] <wave amplitude> <wave period>

%RISER.MATERIAL.SAFETY.FACTORS
<safety class factor>
<material resistance factor>
<buckling propagation factor>
<material strength factor>
<material fabrication factor>
<temperature derating factor for the yield stress>
<temperature derating factor for the tensile strength>

%RISER.NUMBER.SEGMENTS
[number of metallic segments]

%RISER.METALLIC.SEGMENT
[number of metallic segments]
[segment label] [number of segment divisions] <length ratio> <segment length> <concentrated force at the end of the segment> <internal radius> <external radius> <hydrodynamic radius> <riser material> <liner material>

Note: external radius, hydrodynamic radius and riser material are actualized during the optimization, but are included for compatibility with the implementation.

%THICKNESS.VALUES
[number of possible values for thickness]
<list of discrete values for thickness>

%NUM.VAR
[number of surrogate variables]

%NUM.SAMPLES
[number of samples used for model training]

%BETA.MAX
<maximum value for beta from the real function values of the samples>

%BETA.MIN
<minimum value for beta from the real function values of the samples>

%N.FACTOR
<n – E-RBF formulation>

%GAMA.FACTOR
<gamma – E-RBF formulation>

%RADIUS
<radius – E-RBF formulation>

%GAMA.FACTOR
<variables lower and upper bounds>

%CENTERS
<centers – E-RBF formulation>

%WEIGHTS
<weights – E-RBF formulation>

%END